MEASUREMENT OF THE LIFETIME OF THE B_S^0 MESON USING THE EXCLUSIVE DECAY MODE $B_S^0 \rightarrow J/\psi\phi$.

Farrukh Azfar

A DISSERTATION

in

PHYSICS

Presented to the Graduate Faculty of the University of Pennsylvania in Partial Fulfillment of the Requirements for the Degree of Doctor of Philosophy

1996

Supervisor of Dissertation

Graduate Group Chairman

ACKNOWLEDGMENTS

First of all I would like to thank my advisor Professor Nigel Lockyer for his guidance and help, and fostering of a stimulating and egalitarian work environment that made working toward my PhD. one of the most pleasant and challenging experiences of my life.

I would like to thank my friend and colleague Dr Joel Heinrich, one of the very few people from whom one learns something new every day. His patience and kindness were qualities I could always count on. I'd like to thank Professor Larry Gladney the chairman of my committee for all his advice, friendship and patience.

This thesis is dedicated to my family, Abba, Amma, Ayesha and Faisal, without whose love, encouragement and support I could not have completed any of this.

Among my friends at Penn I'd like to thank Anishinder Grewal and his wife Rita for their friendship and affection that pulled me through many a hard day. Among other people in the Physics Department Maneesh, Rahul(tota) and Bindu, Jim, David and Peter. Among friends at CDF I would like to thank Rick Wilkinson, Guillaume Unal, Scott Metzler, Julio Gonzalez, Owen Long, Brendan Bevensee and Chris Holck, among these are some great connoisseurs of the Pakistani language and cuisine ! Our spiritual mentor Wasiq Bokhari is also associated with these fond memories. I'd also like to thank Jeff Cammeretta and Karen Ohl for the cross checks. Among non-Physics people at Penn I'd like to thank Farooq Hamid for all his patient lessons in Farsi, Master Seouk, Alex and the Penn Taekwondo team for helping me maintain a modicum of Physical fitness through my years of graduate work, and last but not

least Ahsan Jameel for all the good times and friendship.

ABSTRACT

MEASUREMENT OF THE LIFETIME OF THE B_S^0 MESON USING THE EXCLUSIVE DECAY MODE $B_S^0 \rightarrow J/\psi\phi$.

Farrukh Azfar

Nigel S. Lockyer

In this thesis a measurement of the lifetime of the bottom-strange meson (B_s^0) in the exclusive decay mode $B_s^0 \rightarrow J/\psi\phi$ is presented. Approximately 100 pb^{-1} of data accumulated at the Fermilab Tevatron during Run-Ia and Run-Ib (1993-1995) have been used. The decay mode is reconstructed completely, making this the only lifetime measurement of the B_s^0 in an exclusive decay mode. The decay $J/\psi \rightarrow \mu^+\mu^-$ is reconstructed and the B_s^0 mass spectrum is extracted by selecting events with a K^+K^- mass consistent with ϕ mass. The lifetime difference between the long (CP odd) and short (CP even) lived components of the B_s^0 has been predicted to be as large as 15–20 %. It has also been suggested that the decay mode $B_s^0 \rightarrow J/\psi\phi$ is predominantly CP even and that the measured lifetime in this mode could be shorter than the lifetime measured in the inclusive decay modes. An observed lifetime difference can be used to extract the $B_s^0 - \bar{B}_s^0$ mixing parameter x_s. This method would not require the tagging algorithms currently in use for B mixing studies. The lifetime of the B_s^0 is measured to be

$$1.34\ ^{+0.23}_{-0.19}\ \text{(stat.)}\ \pm\ 0.05\ \text{(syst.)}\ \text{ps}.$$

This result is currently the best single measurement of the B_s^0 lifetime and is consis-

tent with other measurements of the B_s^0 lifetime. This result is also consistent with measurements of the lifetimes of the B^0, B^+ mesons and the Λ_b baryon. This result is not accurate enough to establish the existence of a possibly significant lifetime difference between the CP odd and even states or consequently the value of x_s.

Contents

List of Tables

List of Figures

شرح این قصه مگر شمع بر آرد بزبان

ورنه پروانه ندارد بسخن پروائ

حافظ شیرازی

Chapter 1

Introduction

In this chapter an overview of the formation of the B_s^0 mesons from $p\bar{p}$ collisions, their decay rates and lifetimes is given. The current world average B_s^0 lifetime from partially reconstructed semi-leptonic decay modes at the DELPHI, OPAL and ALEPH collaborations is $\tau_{B_s^0} = 1.59 \pm 0.11$ ps [1]. A recent CDF measurement by Y.Cen [2] from the semileptonic decay $B_s^0 \rightarrow D_s l \bar{\nu}_l$ is $\tau_{B_s^0}$ =1.42 $^{+0.27}_{-0.23}$ (stat.) $\pm$ 0.11 (syst.) ps. The data used for this result was taken at CDF from 1992-1993 and is designated as the Run-Ia data. This result was published with the exclusive analysis result of $\tau_{B_s^0}$ =1.74 $^{+1.1}_{-0.6}$ (stat.) $\pm$0.07 (syst.) in the fully reconstructed decay mode $B_s^0 \rightarrow J/\psi\phi$ [3]. This thesis describes a further analysis of the exclusive decay mode $B_s^0 \rightarrow J/\psi\phi$ with much higher statistics from data taken at CDF during 1994-1995 (Run-Ib). The current analysis remains the only one of its kind in the world. The decay mode $B_s^0 \rightarrow J/\psi\phi$ is of particular interest due to the fact that a possible predominance of the CP even B_s^0 state could lead to the observation of a lower lifetime relative to measurements in the semi-leptonic modes. A discussion of the x_s mixing parameter and its relation to the lifetime measurement in the decay mode $B_s^0 \rightarrow J/\psi\phi$ is presented

at the end of this chapter.

1.1 Formation of B Mesons in $p\bar{p}$ Collisions

The formation of B mesons in $p\bar{p}$ collisions involves two processes, the first is the production of b quarks from $p\bar{p}$ collisions and the second their hadronization to a particular B meson. A short description of both processes follows.

1.1.1 b–Quark Production in $p\bar{p}$ Collisions

To study the production of quarks from $p\bar{p}$ collisions it is important to remember that every proton (or anti-proton) contains 3 valence quarks and a sea of virtual quark–anti-quark pairs and gluons. The process of b quark production can be thought of as the result of interactions between the parton constituents of the protons and anti-protons. The cross-section is actually an appropriately weighted sum of gluon–gluon, quark–quark and quark–gluon interactions. It has been shown that at high values of the square of the momentum transfer (q^2) the partons (both valence and virtual) may be considered free [4]. Thus the problem of b quark (or any other quark) formation in $p\bar{p}$ collisions can be thought of as a series of interactions in which parton i in a proton reacts with a parton j in an antiproton. These cross-sections are calculated as a perturbative series in $\alpha_s(q^2)$, the QCD coupling parameter. The most important contributions come from order α_s^2 and α_s^3 processes. The Feynman graphs for processes of type $q\bar{q} \rightarrow b\bar{b}$ and $gg \rightarrow b\bar{b}$ (order α_s^2) are given in Figs 1.1 and for processes of type $q\bar{q} \rightarrow b\bar{b}g$, $gg \rightarrow b\bar{b}$ and $qg \rightarrow b\bar{b}g$ (order α_s^3) are given in Fig 1.2. The expression

for the Lorentz-invariant cross-section is given below [5]

$$\mathbf{E}\frac{\mathbf{d^3\sigma}}{\mathbf{d^3k}} = \sum_{\mathbf{i,j}} \iint \mathbf{dx_p dx_{\bar{p}}} (\mathbf{E}\frac{\mathbf{d^3\sigma_{ij}(x_p P_p, x_{\bar{p}} P_{\bar{p}}, \mu)}}{\mathbf{d^3k}}) \mathbf{F_i^p(x_p, \mu) F_j^{\bar{p}}(x_{\bar{p}}, \mu)}, \qquad (1.1)$$

where the sum over indices i and j represents a sum over light partons *i.e.* gluon, up, down, strange and charm quarks (and the corresponding anti-quarks), x_p ($x_{\bar{p}}$) is the fraction of the momentum carried by the ith(jth) parton in the proton(anti-proton), P_p and $P_{\bar{p}}$ are the momenta of the proton and anti-proton respectively, $F_i^p(x_p, \mu)$ and $F_j^{\bar{p}}(x_{\bar{p}}, \mu)$ are the probability distribution functions (evaluated at scale $\mu = q^2$) for the ith (jth) parton in the proton(antiproton) to be carrying a fraction $x_p(x_{\bar{p}})$ of the total momentum of the proton(anti-proton). This expression is thus a sum over all possible free-parton interactions convoluted by the probability distribution functions for the partons to be carrying a particular momentum in the proton or anti-proton. The b production cross-section was first measured at CDF by R. Hughes [6]. The most recent b quark production cross-section measurement at CDF is $\sigma_{p\bar{p}\to bX} = 12.16 \pm 2.07$ μb for b quarks with $P_t > 6$ GeV and rapidity $\mid y \mid < 1.0$ [7]. The b production cross section at LEP from $Z_0 \to \bar{b}b$ is 4.5 nb, at CESR which operates at the $\Upsilon(4S)$ resonance, it is 1 nb. Hence the Tevatron is a promising facility to study B-decays.

1.1.2 Formation of the B_s^0 Meson

Once the b quark is produced it will polarize the vacuum creating quark-antiquark pairs in its path. The created pairs will themselves create more pairs, and as this process continues various hadrons are formed. To get an idea of the likelihood of B_s^0 meson formation in this process it is important to know the probabilities of the

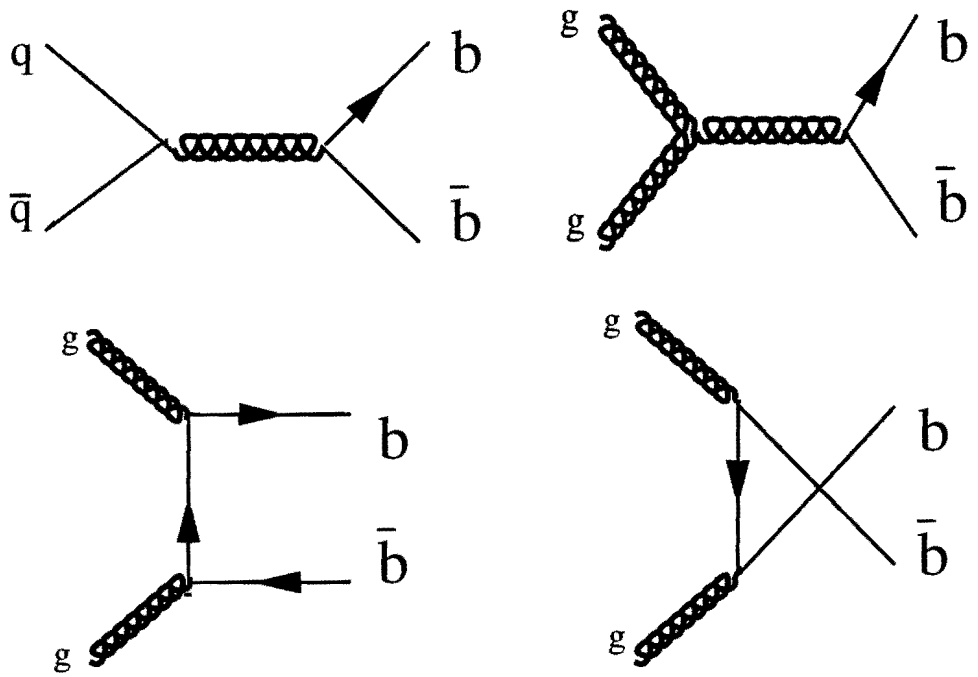

Figure 1.1: Lowest order (α_s^2) processes contributing to b quark production.

formation of different quark-anti-quark pairs. There are many models which describe fragmentation [8] and they assume that the probability of producing a $q\bar{q}$ pair is proportional to $e^{-m_q^2}$ where m_q is the quark mass. Given the existence of a b quark the probability of production of a $b\bar{q}$ state is just the probability of creation of the $\bar{q}q$ pair. The probabilities for a b quark to fragment into various hadrons, taking into account the strangeness suppression factor [9] for the production of $s\bar{s}$ pairs(~ 0.33) are

$$B_u : B_d : B_s : \text{b} - \text{Baryons} = 0.375 : 0.375 : 0.15 : 0.10. \qquad (1.2)$$

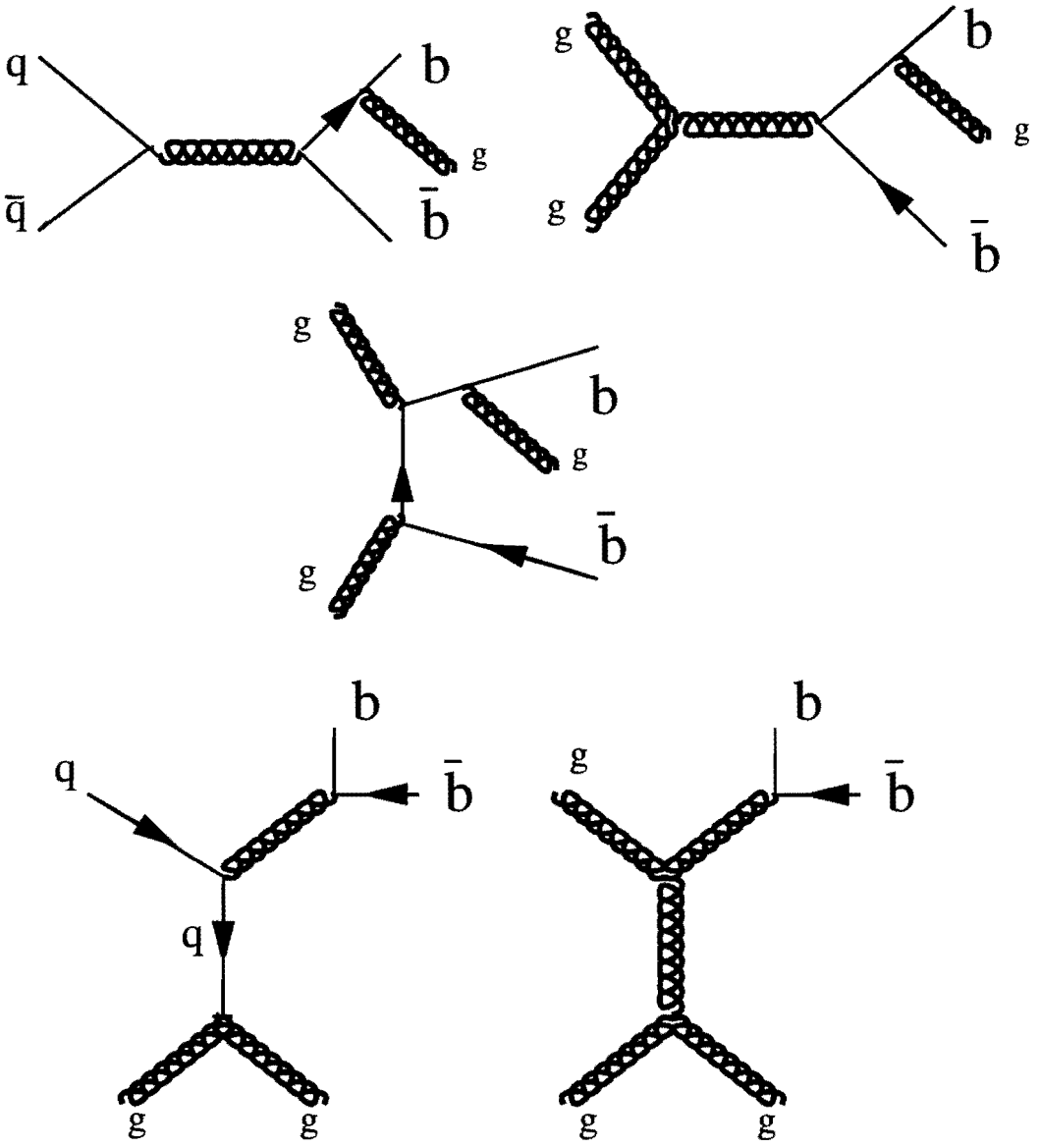

Figure 1.2: Order α_s^3 processes contributing to b quark production.

1.2 Decay of the B_s^0 Meson

A summary of the mechanisms governing the decay of the B_s^0 meson is given. A more detailed discussion of lifetime differences between the CP even and odd states of the B_s^0 meson and its importance follows. The relation of the lifetime difference to mixing in the B_s^0 system is discussed in somewhat more detail.

1.2.1 B Meson Lifetimes

In 1983 the MARK II [10] and MAC [11] collaborations calculated a B-hadron mean lifetime of $\sim$ 1.2 ps from the impact parameter distribution of prompt leptons. This lifetime was an order of magnitude higher than an expected lifetime of $\sim$ 0.07 ps. The implication of the MARK II and MAC results is that the coupling between the second and third generations of quarks is much weaker than that between the first and the second. The lifetime can be used to calculate the magnitude of the CKM matrix element V_{bc} which is an order of magnitude smaller than V_{ud}. The lifetime of a B meson can be approximated to first order by the "spectator" quark model in which the heavier quark inside a meson is assumed to be free. In this approximation the second quark in the meson plays no role in the determination of the lifetime and as such is called a "spectator" quark. Assuming the correctness of the spectator model the width of any B meson (or the b quark) is given by [12]

$$\Gamma = \frac{G_F^2 m_b^5}{192\pi^3}\Big(\sum_{i=u,c}\sum_{j=\bar{u},\bar{c}}\sum_{k=d,s} \mid V_{q_ib}V_{q_jq_k} \mid^2 \Phi(\epsilon_{q_i},\epsilon_{q_j},\epsilon_{q_k}) + \sum_{i=u,c} \mid V_{q_ib} \mid^2 \Phi(\epsilon_q)\Big). \quad (1.3)$$

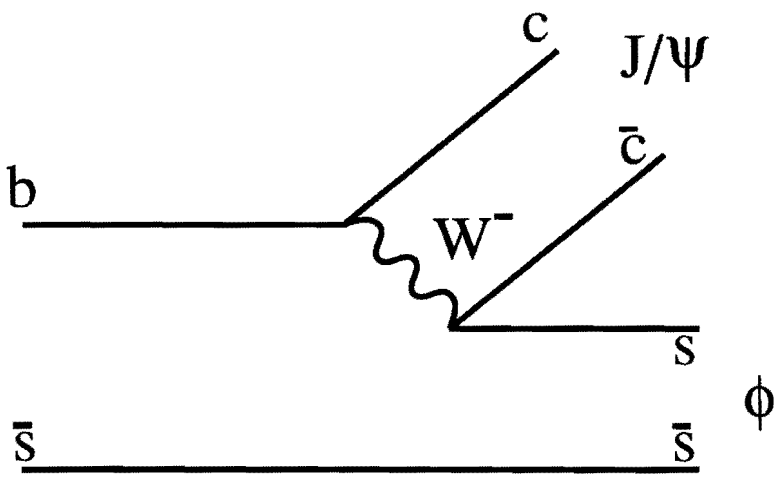

Figure 1.3: Spectator Feynman graph contributing to the process $\bar{B}_s^0 \rightarrow J/\psi\phi$

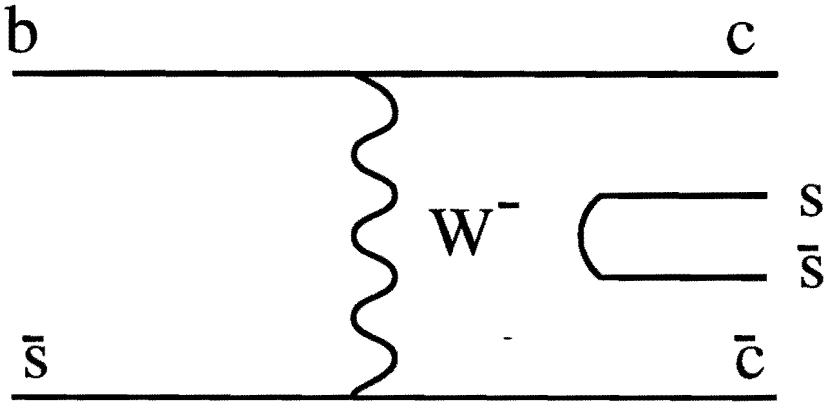

Figure 1.4: Weak annihilation Feynman graph contributing to the process $\bar{B}_s^0 \rightarrow J/\psi\phi$

where the $V_{q_i b}$ are the appropriate CKM matrix elements, m_b is the bottom quark mass, Φ is the phase space factor and ϵ_q is defined as $\frac{m_q}{m_b}$, the first term is from hadronic decays and the second from semi-leptonic decays and the lifetime is given by $\tau_b = \frac{1}{\Gamma}$. In Eqn. 1.3 the index i represents a sum over u and c quarks, and the indices j and k over c, u, s and d quarks. Studies of the momentum spectrum of leptons from b decays [13] [14] have showed that $\mid V_{ub} \mid$ is $\sim 0.1 \mid V_{cb} \mid$. Therefore the lifetime scale of B mesons is set by the magnitude of V_{cb}. The diagram for the spectator-decay of the B_s^0 in the decay mode $J/\psi\phi$ is given in Fig. 1.3.

The spectator model is an approximation and this fact can be seen most clearly in the differences in lifetimes of the various D mesons where,

$$\tau(D^+) > \tau(D_s^+) \sim \tau(D^0) > \tau(\Lambda_c). \tag{1.4}$$

The lifetimes are [32], $\tau(D^+) = 1.057 \pm .015$ ps, $\tau(D_s^+) = 0.467 \pm 0.017$ ps, $\tau(D^0) = 0.415 \pm 0.004$ ps and $\tau(\lambda_c) = 0.2 \pm 0.011$ ps. Since the b quark is much heavier than its partners in mesonic bound-states, the spectator model is a much better approximation than in the D meson system. This model is not complete however, and corrections to it from various sources are listed below:

- Other graphs such as Fig. 1.4 also contribute (less) to the width therefore the B_s^0 lifetime is shorter. This particular graph is termed the "weak-annihilation" graph.

- Different graphs with the same final hadronic states will interfere (Pauli Interference) lowering the lifetime.

A detailed study of these effects is provided elsewhere [15]. Suffice it to say that the average B_s^0 lifetime is predicted to be almost the same as the B_d^0 lifetime. A small difference is predicted between the $B_{d,s}^0$ and the B_u^+ and is given by

$$\frac{\tau(B^+)}{\tau(B_{d,s}^0)} = 1 + 0.05.\frac{f_B^2}{(200MeV)^2}, \tag{1.5}$$

where f_B ($\sim$ 185 $\pm$ 25MeV) is the B_s^0 decay constant. The lowering(increase) in lifetimes(widths) is relative to the charged B mesons. We expect the hierarchy of lifetimes in the B system to follow the pattern observed in the D system. Thus with the replacement $c \rightarrow b$ we have

$$\tau(B^+) > \tau(B_s^0) \sim \tau(B_d^0) > \tau(\Lambda_b).$$

The ratio of the charged B to average neutral B lifetime has been measured by F.Ukegawa [16] to be 0.96 $\pm$ 0.10 (stat) $\pm$0.05(sys). A similar measurement from exclusive decays of B_u^+ and B_d^0 [17] gives a ratio of 1.02$\pm$ 0.16 (stat.) $\pm$0.05 (syst.). Although these ratios are consistent with the theoretical prediction in Eqn. 1.5, more data is needed before it can be confirmed.

1.2.2 Width Differences between CP eigenstates and Mixing in B Mesons

Although it is common in the literature to refer to B mesons as B_q^0 implying the bound state $\bar{b}q$ (where q is the d or s quark), it is important to remember that the physical objects involved in weak interactions are the CP eigenstates formed from linear combinations of $b\bar{q}$ and $\bar{b}q$. Instead of referring to $\tau_{B_d^0}$ as the B_d^0 lifetime, a more appropriate terminology is $\bar{\tau}_{B_d^0}$ *i.e.* the *average* B_d^0 lifetime. This means that a lifetime

measurement in a decay mode that is dominated by either CP eigenstate could be very different from a measurement of one dominated by the other CP eigenstate, or from a decay mode containing a mixture of both. The B_q^0 and $\bar{B}_q^0$ form a 2-state quantum-mechanical system. As in the kaon system it is possible for a B meson to change to a $\bar{B}$ meson through second-order weak interactions represented in perturbation theory by the Feynman "box-diagram". It is therefore useful to consider the CP eigenstates B_1 (CP odd) and B_2 (CP even) defined as

$$\mid B_1 >= \frac{1}{\sqrt{2}}(\mid B > - \mid \bar{B} >), \tag{1.6}$$

and

$$\mid B_2 >= \frac{1}{\sqrt{2}}(\mid B > + \mid \bar{B} >). \tag{1.7}$$

The time evolution of these CP eigenstates is then given by

$$\mid B_i(t) >= \mid B_i(0) > e^{-i(m_i - i\frac{\Gamma_i}{2})t}, \tag{1.8}$$

where i=1 represents the CP odd state and i=2 the CP even state, m_i is the mass eigenvalue and Γ_i the corresponding width. It is important to note that there are two distinct masses and widths corresponding to each CP eigenstate. The probability that a B_q^0 meson will propagate into a $\bar{B}_q^0$ meson over a long period of time is given by,

$$P_{B_s^0 \to \bar{B}_s^0} = \frac{1}{2}(\frac{x_q^2}{1+x_q^2} + \frac{1}{1-y^2})(1-y^2) \tag{1.9}$$

where x_q and y are defined in terms of the m_i and Γ_i

$$x_q = 2\frac{m_1 - m_2}{\Gamma_1 + \Gamma_2} = \frac{\Delta m}{\Gamma} \tag{1.10}$$

$$y = \frac{\Gamma_1 - \Gamma_2}{\Gamma_1 + \Gamma_2} = \frac{\Delta\Gamma}{2\Gamma}. \tag{1.11}$$

The ratio x_q is known as the "mixing parameter".

The difference in the widths of the CP odd and CP even states is denoted by $\Delta\Gamma$ and the average of the CP even and odd state widths is Γ. For B_d^0 mesons the mixing parameter is denoted by x_d and for the B_s^0 by x_s. Several measurements of x_d at various experiments have led to a current world-averaged value of x_d of 0.73± 0.04 [18]. A measurement of mixing in the B_s^0 system by the ALEPH collaboration has put a lower limit of 8.8(95 % CL) on x_s the mixing parameter and a theoretical calculation by A.Ali and D.London [19] has estimated $11.7 < x_s < 29.7$. So far B mixing analyses have relied on tagged samples of B decays, however recently it has been noted [20] that a difference in the widths of CP even and odd states of the B_s^0 could be a hitherto unobserved mixing phenomena leading to a possible measurement of x_s. In the Standard Model the ratio $\frac{\Delta m}{\Delta\Gamma}$ can be calculated with no CKM uncertainties [20]

$$\frac{\Delta m}{\Delta\Gamma} \sim -\frac{2}{3\pi}\frac{m_t^2}{m_b^2}(1 - \frac{8}{3}\frac{m_c^2}{m_b^2})^{-1} h(\frac{m_t^2}{M_W^2}), \tag{1.12}$$

where $h(y) = 1 - \frac{3(1+y)}{4(1-y^2)}(1 + \frac{2y}{1-y^2}\log(y))$. Therefore x_s can be expressed as

$$x_s = -\frac{\Delta\Gamma}{\Gamma}\frac{2}{3\pi}\frac{m_t^2}{m_b^2}(1 - \frac{8}{3}\frac{m_c^2}{m_b^2})^{-1} h(\frac{m_t^2}{M_W^2}). \tag{1.13}$$

1.2.3 The Decay mode $B_s^0 \to J/\psi\phi$ and the Measurement of x_s

Although no conclusive experimental evidence is available, many theorists have conjectured that the decay mode $B_s^0 \to J/\psi\phi$ is dominated by the CP even state [21].

A measurement of the ratios of longitudinal *vs* transverse polarizations of the decay mode $B_s^0 \rightarrow J/\psi\phi$ [22] has given a ratio of $0.56 \pm 0.21(\text{stat}) \pm 0.03$ which is consistent with this decay mode containing a mixture of both CP states or with its being completely CP even. It is possible that the best guess of the CP content of this decay mode can be made by looking at the CP content of the decay mode $B_d^0 \rightarrow J/\psi K^*(892)^0$. The results here are not conclusive but the world average of 0.74 ± 0.07 tells us that at least 60 % of it is CP even at the 90% confidence level [22]. The conclusion of this analysis provides a hint (Chapter 7, Conclusion) that the lifetime in this decay mode is lower than what the average B_s^0 lifetime is expected to be. However a larger data sample is needed to establish this conclusively. Unfortunately an accurate measurement of x_s is not possible with the current data sample and it is hoped that higher statistics in Run-II (beginning 1999)will result in an accurate measurement of x_s using this method.

Chapter 2

CDF detector

This chapter briefly describes the Fermilab Tevatron and the CDF detector. A general overview of the Tevatron and the entire detector is followed by a more detailed discussion of the Muon Chambers, the CTC, VTX and the SVX, these are the detector components most relevant to the analysis described in this thesis.

2.1 The Fermilab Tevatron

The Fermilab Tevatron is a $p\overline{p}$ collider operating at a center of mass energy of 1.8 TeV and is the highest energy collider in the world. A plan view of the Tevatron is shown in Figure 2.1. More detailed descriptions of the Tevatron are given elsewhere [23] [24]. A brief description of its operation follows:

Protons are extracted from a bottle of hydrogen gas and ionized to form H^- ions. These H^- ions are first accelerated in a Cockroft-Walton accelerator to 750 keV and then in a 150 m long linear accelerator (LINAC) to an energy of 200 MeV. The 2 electrons are then stripped off of the ions and the resulting protons are accelerated in 475 m circumference circular accelerator known as the Booster. At the end of this

stage the protons have an energy of 8 Gev and are grouped into 6 bunches of roughly $2x10^{10}$ protons each. The protons are then transferred to the Main Ring which is a circular accelerator of circumference 6.3 km, here all the bunches are combined into one bunch of roughly $7x10^{10}$ protons and are accelerated to 150 GeV. Below the Main Ring with the same circumference of 6.3 km is the Tevatron into which protons are transferred and accelerated to 900 GeV. The crossing time is roughly 3.5 μs.

The procedure for anti-protons is different because they are created at a relatively high energy. Protons at 120 GeV are extracted from the Main Ring and redirected toward a copper target and the anti-protons are created as a result of the collisions. Antiprotons with energy near 8 GeV are selected and then put into the Main Ring from where they are sent into the Tevatron. They are then accelerated to 900 GeV and so the lab frame is also the center of mass frame with an energy of 1.8 TeV. All of this energy is not available for particle creation since this energy is distributed among the parton constituents of the protons and anti-protons. The energy available for creation of particles in any one parton-parton collision is 300 GeV.

2.2 A brief overview of the CDF Detector

The CDF detector is designed to study physics in the Tevatron environment at Fermilab. The detector surrounds the interaction point with azimuthal and forward–backward symmetry. An isometric view of the detector is provided in Fig. 2.2.

Three tracking chambers surround the beam-line in succession. The inner-most chamber is the SVX (Silicon Vertex Detector) which provides high-precision vertex

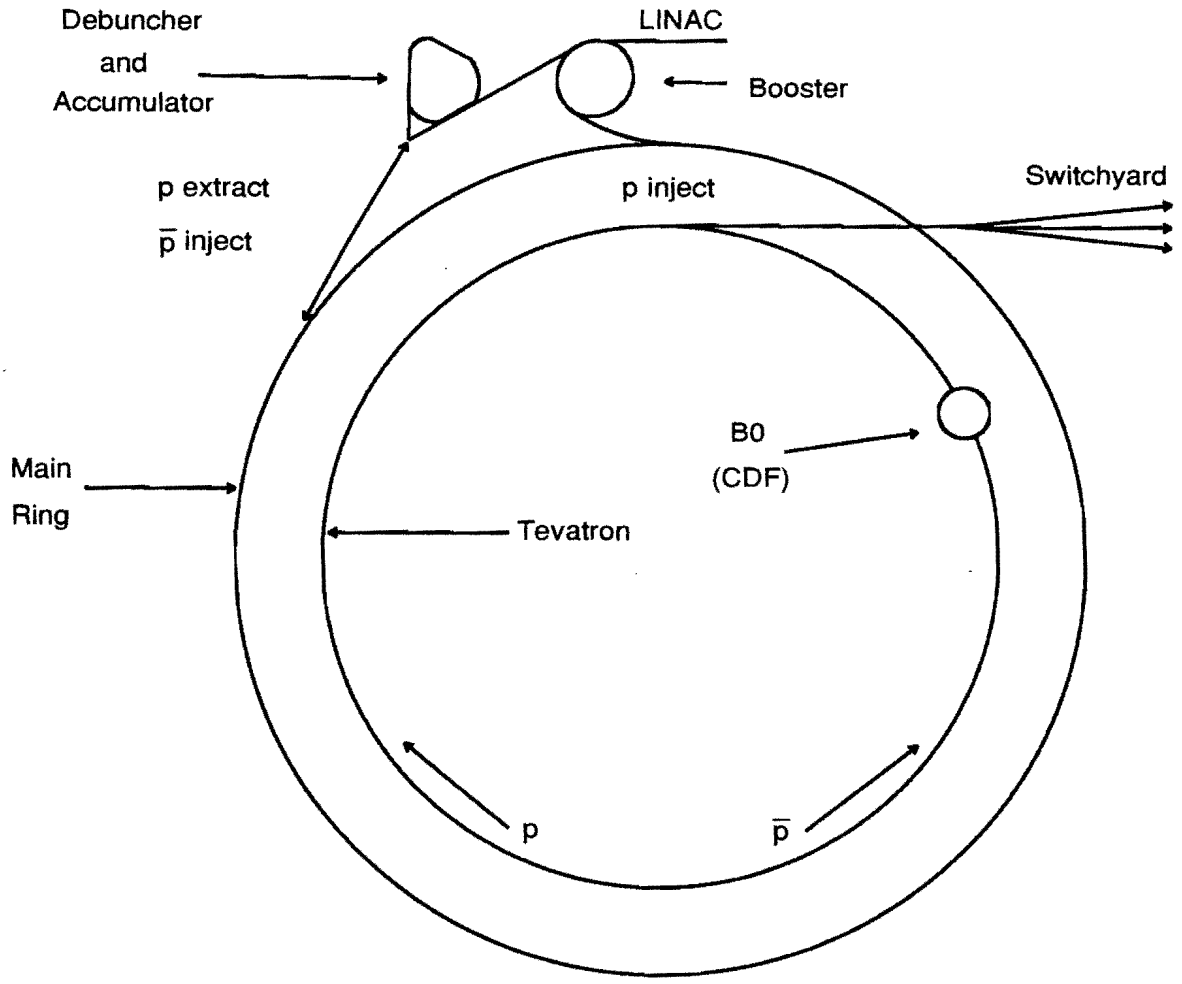

Figure 2.1: A plan of the Tevatron and the position of CDF (B0 collision point).

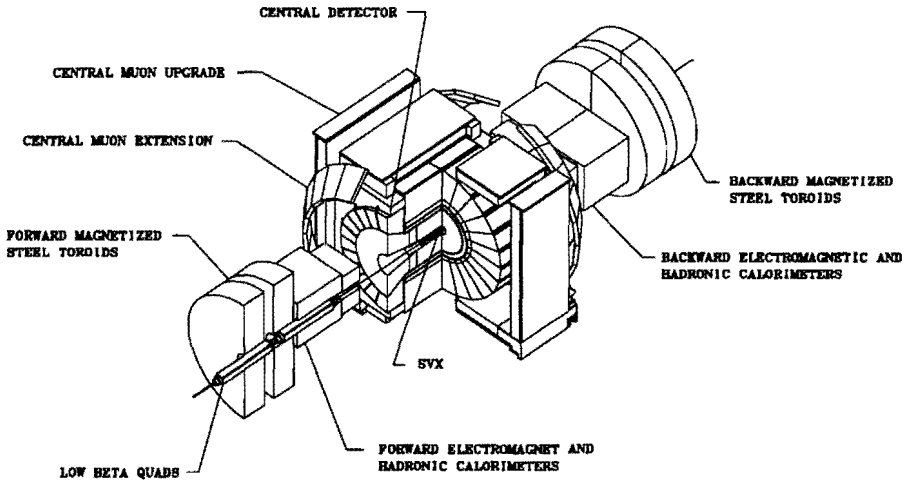

Figure 2.2: An isometric view of the CDF detector.

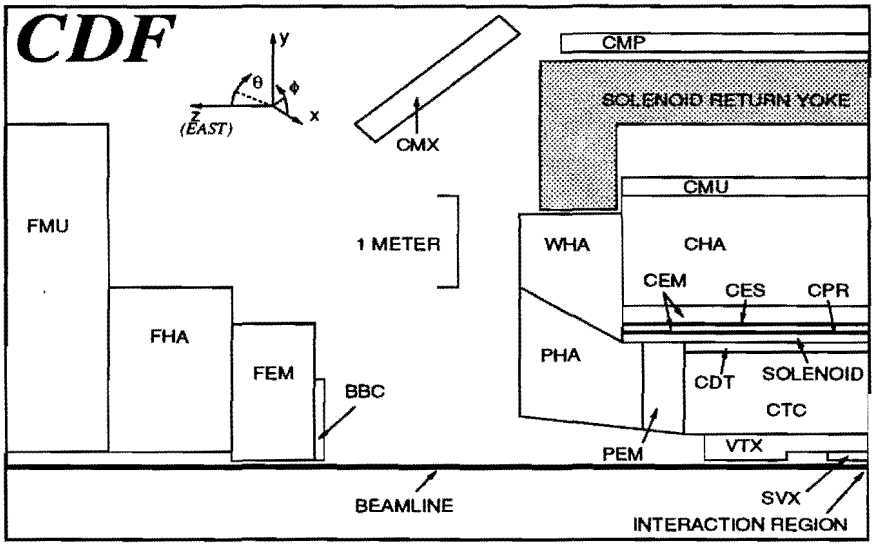

Figure 2.3: A side view of the CDF detector

measurements. The next chamber is the VTX which measures positions of vertices in z. The third chamber is the CTC (Central Tracking Chamber) which surrounds the previous two and provides tracking both in the r-ϕ plane and in the z-coordinate. This entire central region is surrounded by a superconducting solenoid of radius 1.5 m and length 4.8 m and provides a 1.5 Tesla magnetic field in the z direction (Fig. 2.3). Outside the tracking chambers and the solenoid are various calorimeters and the muon drift chambers. The Calorimetry consists of the CEM, CHA and the FEM and FHA (Central Electromagnetic, Central Hadronic, Forward Electromagnetic and Forward Hadronic). These measure the electromagnetic and hadronic energies of photons, electrons and hadrons. Surrounding the calorimetry are the muon drift chambers, the CMU, CMP, CMEX and the FMU (Central Muon, Central Muon Upgrade, Central Muon Extension and the Forward Muon chambers) (Figs 2.3 2.2). These chambers (with the exclusion of the FMU) are crucial to this analysis since the detection of this (and several other B meson exclusive modes) decay modes have a J/ψ as a decay product. The Level 2 dimuon trigger relying on the muon chambers allows the detection of events with the J/ψ in the decay mode $J/\psi \rightarrow \mu^+\mu^-$, at present there is no trigger for di-electrons.

2.3 Silicon Vertex Detector

Since B mesons are long lived they decay away from the primary vertex at a secondary vertex which is still within the 1.9 cm radius beryllium vaccum pipe. Isolating them requires a precision vertex detector capable of identifying vertices displaced from the

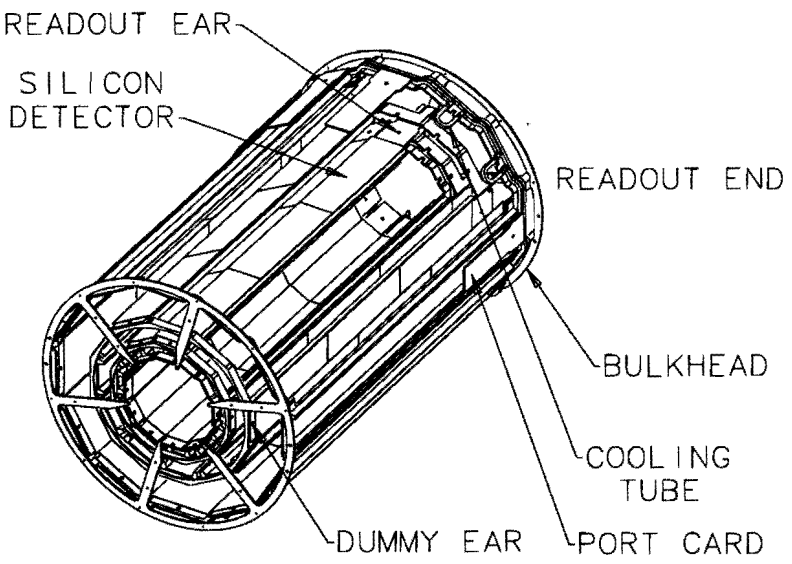

Figure 2.4: A sketch of one of two SVX barrels

primary. The SVX is such a detector installed at CDF in 1992 and is designed for the purpose of identifying secondary vertices. This was the first time such a detector was installed at a hadron collider [25].

The SVX has four radial layers of silicon microstrips. The radial distance of the innermost layer from the beam is 3 cm, the final layer is at 7.9 cm. There are two modules consisiting of 4-concentric layers that are 12-sided barrels. Each side is thus the edge of a "wedge" subtending an angle of 30° in the $r - \phi$ plane at the z-axis. The two modules have a gap of 2.15 cm between them and together have a length of 51 cm. Since the z co-ordinate of the $p\overline{p}$ collision point lies anywhere along a line 30 cm long, the actual coverage of the SVX is about 60 %. A picture of one such module (barrel) is given in Figure 2.4.

Each silicon strip detector consists of a 300 μm thick silicon single crystal parallel

to the beam axis (z-axis). A series of strips traverse these crystals with a pitch depending on the layer of the SVX (Table 2.1). Three such detectors are electrically wire-bonded together to form an SVX 'ladder'. A ladder traverses the entire length of one barrel. One such ladder is illustrated in Figure 2.5. Each strip is read out at the end of the ladder.

Table 2.1: SVX geometry constants for any 30 ° wedge.

Layer	Radius (cm)	Thickness (μm)	Pitch (μm)	Number of Readout strips
1	3.005	300	60	256
2	4.256	300	60	384
3	5.687	300	60	512
4	7.866	300	55	768

The details of the SVX Geometry including strip pitches for each layer etc. are given in table 2.1.

2.4 VTX

Outside the SVX is a time projection vertex chamber (VTX), installed in 1992, which provides the measurement of the $p\overline{p}$ interaction vertex along the z. Its outer radius is 22 cm and tracks reconstructed here are matched to tracks in the CTC (Central Tracking Chamber) chamber with its z measurement. The VTX is composed of 8 modules, has 8 octants and each octant has 24 sense wires. Each module is divided

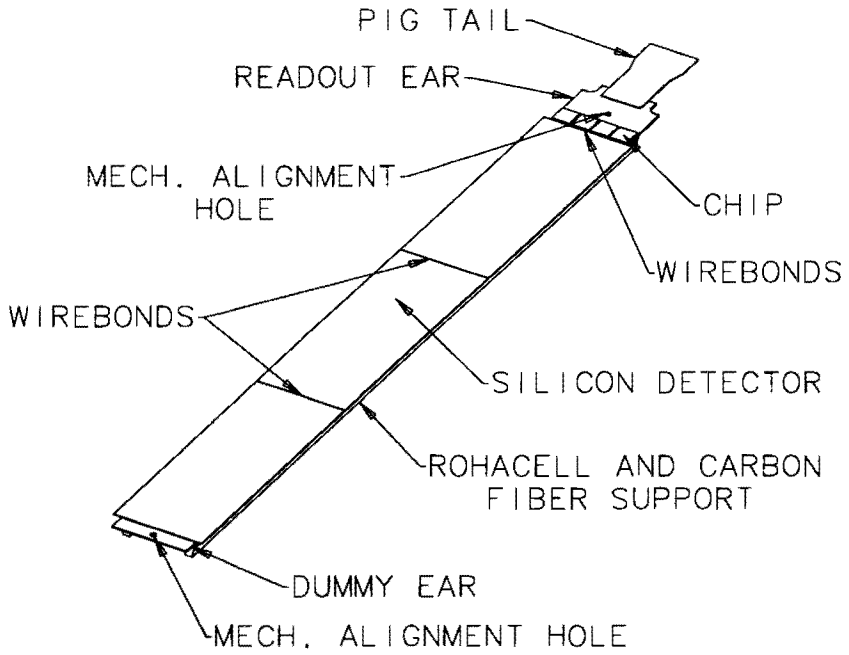

Figure 2.5: A drawing of 3 silicon-strip detectors joined together to form an SVX ladder.

into 2 drift regions and thus there are a total of 3072 sense wires. The VTX is filled with an argon-ethane gas mixture and has a resolution of 1 mm in z. The positioning of the wires and the divsion into modules corresponds to a drift time of 3.3 μs.

2.5 Central Tracking Chamber

The CTC is a large cylindrical drift chamber of length 3.2 m and outer radius 1.3 m. The CTC lies outside the VTX. An illustration is given in Figure 2.6 The CTC measures the track parameters of charged tracks from which the momentum of the tracks are calculated. It consists of 9 super layers of sense wires. The axial wires are in the superlayers numbered 0, 2, 4, 6, 8 and are used to determine r and ϕ information. The superlayers 1, 3, 5, 7 are stereo layers which extract information

in r and z. Alternate stereo layers make an angle of $\pm$ 3 ° with the beam line. The axial wires have 12 wires per cell and the stereo 6; thus there are 84-layers of wires in all. The chamber is filled with a mixture of argon-ethane in equal proportions. The spatial resolution for a single hit in r-ϕ is 200 μm and 6 mm in z. The division into cells translates to a drift time of $\sim$ 800 ns.

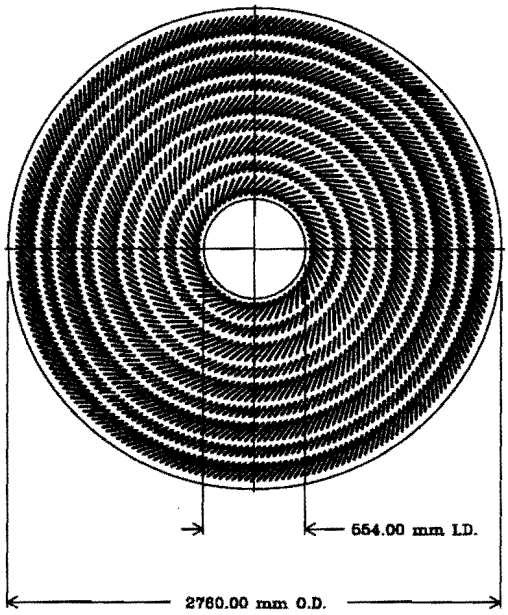

Figure 2.6: End view of the Central Tracking Chamber showing the superlayers and the cells

2.6 The Muon Detectors

2.6.1 The Central Muon Chambers (CMU)

The Central muon chambers lie outside electromagnetic and hadronic calorimetry, a muon traversing this portion of the detector has already travelled $\sim$ 6 interaction

lengths. The CMU consists of 48 wedges surrounding the calorimetery, each wedge subtends an angle of ϕ=12.6° at the z-axis, there is a gap of 1.2 ° at either side of each wedge.

Each wedge contains 3 chambers as shown in Figure 2.7. The chambers contain four cells in alternating layers each with a sense wire. The trajectory of the muons in the chambers is a straight line. A hit on a wire can be thought of as coming from an ionization on the left or right. To resolve this ambiguity the sense wires in each cell are staggered in position by a known amount.

A charge division readout gives a z position. The chambers measure four points along the muon's track, these positions are then fit to straight line in the $x - y$ and $y - z$ planes. This resulting "stub" is matched to all charged tracks in the CTC that can be extrapolated to this chamber and the track with the lowest χ^2 of the match is accepted as a muon candidate. The quality of this match is a quantity that we cut on later as well. The coverage of the Central Muon Chambers is $\pm$ 0.6 η.

2.6.2 The Central Muon Upgrade (CMUP)

To further reduce the probability that a candidate muon track is due to hadronic punch-through an additional set of chambers has been added behind the steel shielding surrounding the detector. A particle associated with a stub in this system has already traversed 8 interaction lengths. The CMUP covers most of the same range in η as the CMU. There is no trigger associated with the CMUP and this system serves to increase confidence that a track is actually a muon.

2.6.3 The Central Muon Extension (CMEX)

The Central Muon Extension increases the coverage in η to $\pm$ 1 (CMU+CMP cover $\pm$ 0.6) and lies between $0.6 < | \eta | < 1$. About a tenth of all muons are detected in the CMEX.

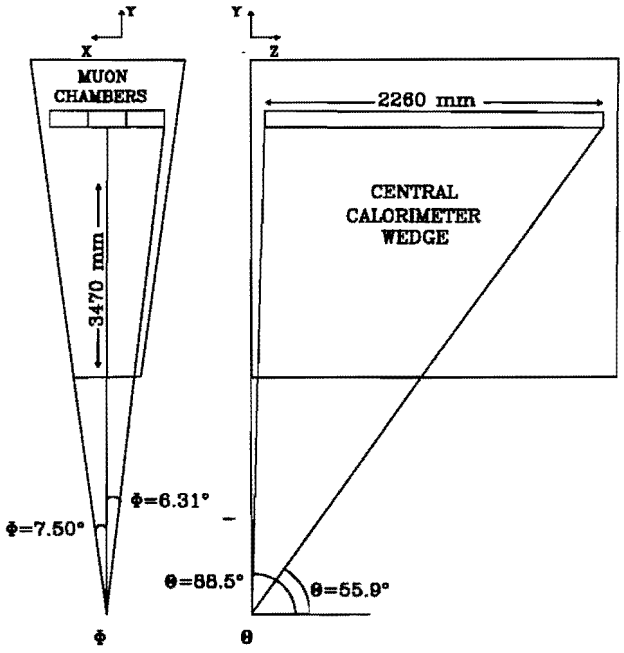

Figure 2.7: A picture of a 12.6 ° wedge of the CMU system.

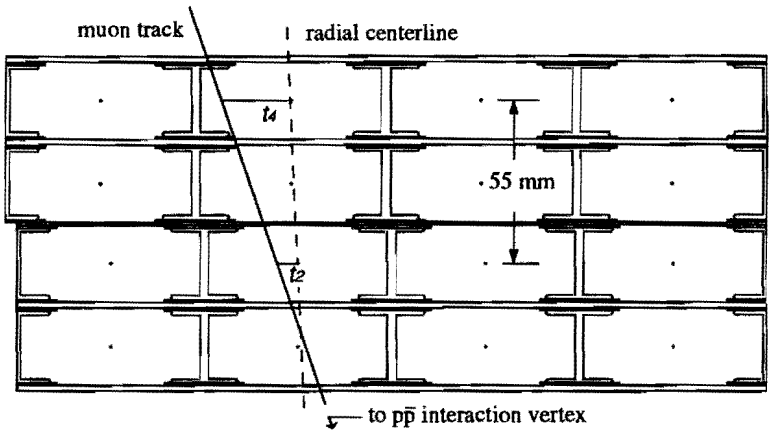

Figure 2.8: An illustration of a single chamber of the Central Muon Chamber. The drift time to layers 2 and 4 is shown.

Chapter 3

Tracks, Vertices and Decay Lengths

An accurate measurement of the distance traveled by the B_s^0 meson before decaying requires a precise knowledge of the track parameters of the charged daughters, the position of the primary interaction vertex, the position of the decay of the B_s^0 (secondary vertex), and the errors in measuring each of these. For the analysis of the decay $B_s^0 \rightarrow J/\psi\phi$ where $\phi \rightarrow K^+K^-$ and $J/\psi \rightarrow \mu^+\mu^-$, the 2 muons are required to have traversed both the SVX and the CTC, therefore at least half of all tracks used have their parameters determined through the use of more than one detector. Information from successive detector components along a particle's trajectory can be used in a sequential fitting technique to determine the track parameters. This method is implemented in the CDF tracking software. The next 3 sections briefly describe the reconstruction of tracks in the Muon Chambers, the CTC and the SVX. This is followed by a brief explanation of the procedure of progressive track fitting involving the use of information from more than one detector to determine the path of a charged particle. Finally the calculation of the proper-decay length of B_s^0 mesons is described.

3.1 Tracks

The purpose of this section is to describe briefly the tracking algorithm in use at CDF. Also listed are the track selection cuts imposed in each detector.

3.1.1 Detection of muons in the Muon Chambers

The Muon Chambers have been described in Chapter 2 (The CDF Detector). Muons are minimum-ionizing particles and lose little energy when traveling through matter. Therefore they can be distinguished from other particles by their ability to travel further through matter. The muon chambers are therefore located outside the bulk of detector material and it is assumed that a particle getting through the calorimetry and the steel magnet yoke is a muon. At a later stage the decay mode $J/\psi \rightarrow \mu^+\mu^-$ is explicitly reconstructed with extremely low background further increasing confidence that the tracks used were muons. The presence of an efficient di-muon trigger reduces the combinatoric background that would be present if there were no muon-identification, since then it would be necessary to form combinations between all oppositely charged track pairs in an event and treat the invariant mass as the J/ψ candidate mass. Since the Muon chambers are outside the CDF magnetic field the reconstructed track is a straight line (known as a "stub") in the x-y and x-z planes. Candidate CTC tracks are extrapolated to the muon chambers and a χ^2 is calculated using the errors from the CTC track parameters and an extrapolated CTC track. The muon-quality cuts are listed below:

- χ^2 is < 9 for matching in x-y

- χ^2 is < 12 for matching in z.

3.1.2 Tracking in the CTC

The trajectory of a charged particle in a magnetic field is a helix and is described by 5 parameters. The choice at CDF is $(c, \phi_0, \cot\theta, d_0, z_0)$, a description of each is given below:

- c is the signed curvature of the track, $c = Q.\frac{1}{2r} = \frac{0.00014986B}{P_t}$, where r is the radius of the circle in the x-y plane, B is the magnetic field in Kilogauss, P_t is the transverse momentum of the track in GeV and Q is the charge of the particle($= \pm 1$).

- $\cot\theta$ is the cotangent of the angle of dip and is $= \frac{P_z}{P_t}$, where P_z is the component of momentum in the z direction.

- d_0 is the distance of closest approach of the track to the origin in the x-y plane.

- z_0 is the z co-ordinate of the point of closest approach of the track to the origin.

- ϕ_0 is the angle made by the direction of the track to the x-axis at the point of closest approach in the x-y plane.

The CTC track finding algorithm described below fits for these parameters and if at a later stage compatible hits in the SVX are found, the track is refit and the parameters recalculated. The track finding algorithm in the CTC begins by grouping all hits on

wires in each superlayer cell into line segments. Since the outer superlayer is the least occupied the algorithm begins here and moves in to the next superlayer along a line to the inner-most layer. A search for line segments that can be matched with the previous and next superlayers is made as the process continues. At the end of this process a group of line segments consistent with coming from a single track have been found and a preliminary fit to a circle in the x-y plane is done. This allows a first measurement of the track parameters c, ϕ_0 and d_0. After this all the hits in the stereo layers that can be associated with this track are found and fit providing a first measurement of the parameter z_0 and $\cot\theta$. In this procedure the χ^2 and track parameters are updated each time a new line segment is found. To ensure a good track quality the following cuts are imposed on every CTC track.

- Each track used must have ≥ 4 hits in each of at ≥ 2 CTC axial superlayers.
- Each track must have ≥ 2 hits in each of ≥ 2 CTC stereo superlayers.

3.1.3 Tracking in the SVX

Tracks that can be extrapolated to the vicinity of a hit-cluster in the SVX are followed into the SVX. The SVX provides information only in the r-ϕ plane. It however improves the measurement of d_0 and ϕ_0 greatly and as such is indispensable to any B lifetime analysis. Although the track finding procedure in the CTC has been described in a separate section, tracking in the SVX can be thought of as a continuation of the CTC tracking into a more accurate detector. A search is made inward from the CTC track into the SVX and any hit-cluster compatible with the extrapolated track

is used into the fit. Each time a new hit-cluster is found the χ^2 is updated and the track parameters are recalculated. This method allows for the effects of multiple scattering to be taken into consideration *locally*, thus correctly accounting for possible deviations in the path of the particle and the association of further points with it. This way only 5 free parameters are fit at each update, and the complicated task of global pattern recognition is avoided. By adding at least 2 more data points and extending the lever-arm of the tracking by ~30cm the SVX-CTC fit improves the track P_t resolution considerably. This analysis requires 3 or 4 hit SVX tracks, even though tracks with 2 hits are available. The ratio $\frac{\sigma_{P_t}}{P_t}$ improves when a CTC fit is combined with information from the SVX

$$\frac{\sigma_{P_t}}{P_t} = 0.0011 + 0.0014 P_t, \tag{3.1}$$

for the CTC only, and

$$\frac{\sigma_{P_t}}{P_t} = 0.0024 + 0.00044 P_t, \tag{3.2}$$

for the CTC+SVX fit. The impact parameter resolution of the SVX as a function of the P_t of the track is given by

$$\sigma_D(P_t) = A + \frac{B}{P_t}, \tag{3.3}$$

here $A \sim 10\mu$m represents the intrinsic detector resolution and $B \sim 41\mu$m-GeV, is the contribution from multiple scattering. The SVX has four concentric layers surrounding the beam-pipe and so 2, 3 or 4 hit-clusters can be associated with a track. The parameters of a track formed with 2 hit-clusters are less well determined

than those with 3 or 4. In Run-Ia statistics were low so SVX tracks with 2 hits were used. In Run-Ib with statistics enhanced by a factor of ~4, and a more efficient SVX it is possible to demand that tracks have 3 or 4 hits and still have a large enough sample to fit. The SVX χ^2 distribution for 4-hit tracks is shown in Fig. 3.1 fitted to the function $F(x) = \frac{x^{0.5n-1}e^{-0.5x}}{2^{0.5n}\Gamma(0.5n)}$ where $x = \chi^2$ and $n = 4$(= number of degrees of freedom= number of hits).

For Run-Ia the quality cuts used for SVX tracks the following:

- For every track for which the SVX-CTC fit is used the number of hits is greater than or equal to 2.
- $\frac{\chi^2}{N}$ is < 6 where N is the number of hits on the particular track and χ^2 is the increment in χ^2 from adding the SVX hits.
- The number of strips fired in each cluster is less than four.

For the Run-Ib and Run-Ia combined analysis the following track quality cuts were used for SVX tracks:

- Number of hit-clusters used is ≥ 3.
- The probability P(χ^2) is > 0.01, where the χ^2 is the increment in χ^2 from adding the SVX hits.
- Both muons have SVX tracks satisfying the preceding requirements.

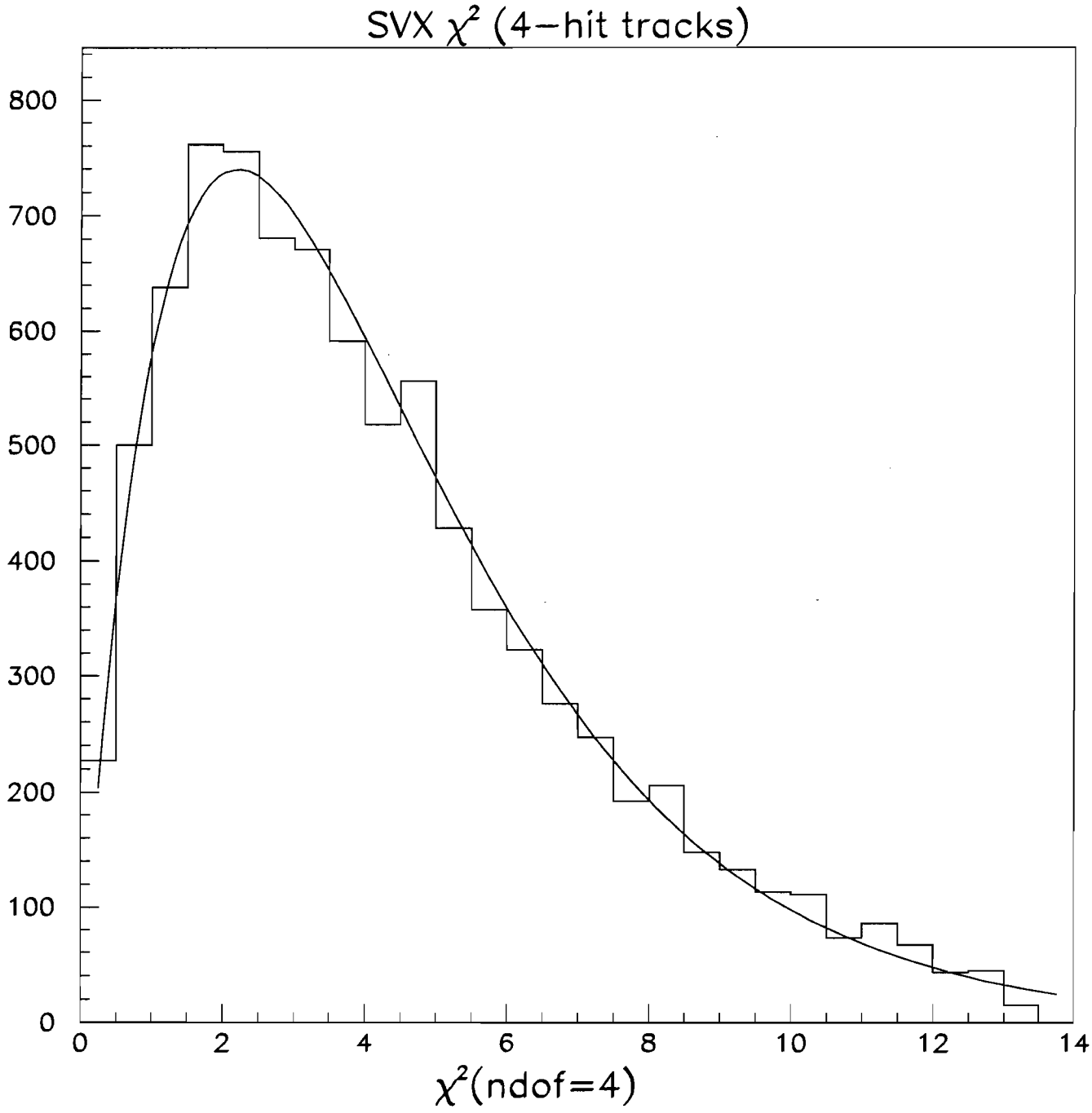

Figure 3.1: SVX χ^2 distribution is shown fitted to the function given in the text.

3.2 Vertices and the Proper Decay length

The procedure for determining the primary interaction vertex and the position in space of the decay of the B meson is described. This is followed by a description of the calculation of the proper-decay length and its error. The description of vertexing and the proper-decay length is valid for a variety of analyses involving the measurement of exclusive lifetimes from neutral B meson decays.

3.2.1 The Primary Vertex

An accurate knowledge of the primary vertex is crucial to the determination of the proper decay length of long-lived particles. The CDF database contains an average beam position for each run. This value is based on SVX measurements and is calculated offline. The determination of the beam position is done on a run-by-run basis using the so called "$D - \phi$" correlation method [33] and a brief description follows. The impact parameter of tracks can be expressed in terms of the position of the primary vertex in the following way

$$D(\phi_0, z_0) = x_0 \sin\phi_0 + m_x \sin\phi_0 z_0 - y_0 \cos\phi_0 z_0 - m_y \cos\phi_0 z_0, \tag{3.4}$$

where x_0 and y_0 are the x and y positions of the primary vertex and m_x and m_y are the slopes of the beam in x-z and y-z planes respectively. The parameters of interest are x_0, y_0, m_x and m_y. The difference between $D(\phi_0, z_0)$ and D_i, the *measured* impact parameter of the ith track, is used to determine the beam position: First it is convenient to define the vectors $\vec{x} = (x_0, y_0, m_x, m_y)$ and $\vec{g} =$

$(\sin\phi_0, -\cos\phi_0, \sin\phi_0.z_0, -\cos\phi_0.z_0)$. The parameters are determined by minimizing the χ^2

$$\chi^2 = \sum_{i=1}^{N} (\frac{D_i - \vec{x}\cdot\vec{g}}{\sigma_i})^2. \tag{3.5}$$

This procedure returns a best fit primary vertex position in (x, y, z). The uncertainty is largest for the beam position in z, however the z-position of the J/ψ is considered to be a good approximation. The x and y beam positions are then corrected using the slopes in x-z and y-z and the z position of the J/ψ

$$x = m_x.x_{fit} + z_{J/\psi} \tag{3.6}$$

$$y = m_y.y_{fit} + z_{J/\psi}. \tag{3.7}$$

$$\tag{3.8}$$

where $z_{J/\psi}$ is the z co-ordinate of the decay point of the J/ψ and x_{fit} and y_{fit} are the fit values of the x and y beam positions. To check for the stability of the primary-vertex position over the course of a run, the fit is repeated every few 100 events and the average deviation is recorded. The variation is 5 μm in x and 8 μm in y. These deviations are taken into account as a possible source of systematic error in the lifetime. A plot of the x beam position, and the x beam position as a function of the z beam position is shown in Fig 3.2.

3.2.2 The Secondary Vertex

After selection of the four candidate tracks, it is necessary to determine if they are consistent with coming from one point in space (secondary vertex) where the decay of

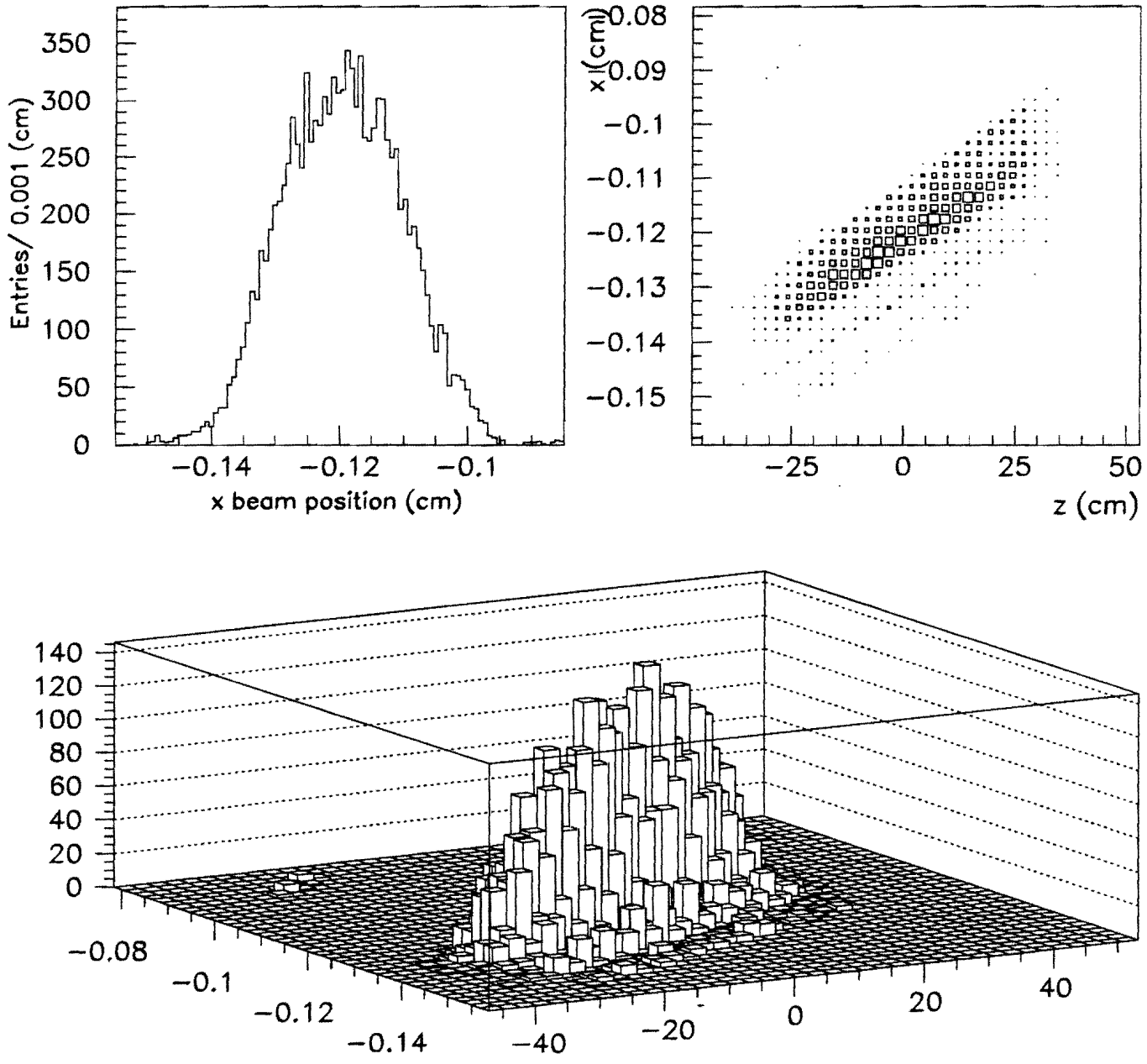

Figure 3.2: The primary vertex position in x is in the plot at top left. A plot of the x *vs* z position is shown (top right). A lego plot of the x position *vs* the z position is shown in the bottom row.

the candidate B_s^0 meson has taken place. The technique used is the vertex-constraint *i.e.*, the 4 tracks are constrained to originate from a single point in space. The track parameters of all 4 tracks and the co-ordinates of the point in space are assumed to be variables. The goal is to minimize the χ^2

$$\chi^2 = \sum_{i,j=1}^{N} \eta_i^t G_{ij}^{-1} \eta_j, \tag{3.9}$$

where $\vec{\eta}$ is the 5 component vector of differences between the unconstrained (measured) track parameters and the recalculated track parameters subject to the vertex constraint and **G** is the calculated error matrix which takes into account the effects of multiple scattering. A crucial factor in finding the best intersection point is the choice of the initial point where the iteration begins. The two intersection points of the projections of the first 2 tracks onto the the r-ϕ plane (circles) are found and the starting point for the iteration is then assumed to be the solution corresponding to the least separation in z. This vertex-constraining procedure is implemented in the CDF software as a user callable subroutine. While performing the 4-track fit the 2 muon tracks are constrained to have the world average mass of the J/ψ [32]. This improves the mass resolution of the B_s^0 considerably. The probability of the vertex constrained χ^2, $P(\chi^2)$, is required to be larger than 1% for 6 degrees of freedom.

3.2.3 The Proper Decay length

The candidate secondary and primary vertices are then used to compute the proper decay length of the candidate B meson. The fit returns the position of the secondary

vertex $\vec{x_s}$ and the associated error matrix $\mathbf{V^{(s)}}$. Already available are the same quantities for the primary vertex $\vec{x_p}$ and $\mathbf{V^{(p)}}$. The momentum of the candidate B meson is calculated using the recalculated track parameters after all constraints. Since at CDF the positions in z of any vertex is the quantity with the largest error, lifetime analyses avoid the use of this co-ordinate and instead rely on measurements purely in the transverse plane. The decay-length measured in the laboratory frame is given by

$$d_{lab} = (\vec{x_s} - \vec{x_p}) \cdot \hat{p}_t, \tag{3.10}$$

where $\hat{p}_t$ is the unit vector in the direction of the transverse momentum of the candidate B meson. The distance traveled in the transverse plane in the B mesons own frame ($=c\tau$ the proper decay length) is given by

$$c\tau = d_{lab}\frac{M_B}{P_t}, \tag{3.11}$$

where M_B is the invariant mass of the candidate B meson. Since the error in P_t is very small the error on this quantity in terms of $\hat{p}_t$, $\mathbf{V(s)}$ and $\mathbf{V^{(p)}}$ is

$$\delta_{c\tau} = \sqrt{(\sum_{i,j=1}^{N} \hat{p}_{t_i}(V_{ij}^{(s)} + V_{ij}^{(p)})\hat{p}_{t_j})}.\frac{M_B}{P_t}. \tag{3.12}$$

Chapter 4

Reconstruction of Exclusive Modes

In this chapter a description of the method used for the reconstruction of exclusive decay modes is given. The decay mode $B_d^0 \rightarrow J/\psi K^*(892)^0$ with $J/\psi \rightarrow \mu^+\mu^-$ and $K^{*0}(892) \rightarrow K^{\pm}\pi^{\mp}$ has three of four daughters in common with $B_s^0 \rightarrow J/\psi\phi$ ($J/\psi \rightarrow \mu^+\mu^-$ and $\phi \rightarrow K^+K^-$) and its reconstruction is used as test of the B_s^0 decay mode.

4.1 Reconstruction of $B_s^0 \rightarrow J/\psi\phi$

The decay chain for the B_s^0 decay is $B_s^0 \rightarrow J/\psi\phi$ with $J/\psi \rightarrow \mu^+\mu^-$ and $\phi \rightarrow K^+K^-$. In each event 2 oppositely charged muon tracks are found and their invariant mass is reconstructed with the 2 tracks constrained to a common vertex using the vertex-constraining algorithm described in Chapter three. If this reconstructed dimuon-mass is within $\pm$ 0.08 GeV of the world average J/ψ mass of 3.097 GeV [32] the invariant mass of all oppositely charged track pairs that are not muons (within this event) is reconstructed with each track assigned the mass of a kaon. If the invariant mass of this 2-track combination lies within $\pm$ 0.01 GeV of the world-average ϕ (1.01943

GeV) [32] mass the invariant mass of this 4 track combination is calculated from the expression

$$M_{invariant} = \sqrt{(\sum_{i=1}^{4} E_i)^2 - \sum_{i}^{4} \vec{P}_i \cdot \sum_{i}^{4} \vec{P}_i}, \tag{4.1}$$

where $\vec{P}_i$ is the 3-momentum of the ith track, E_i is the energy computed from the mass and 3-momentum of the track. The error on this quantity is given by

$$\delta_M = \sqrt{\sum_{i,j}^{5} \frac{\partial M}{\partial \alpha_i} V_{ij}^{(s)} \frac{\partial M}{\partial \alpha_j}}, \tag{4.2}$$

where α_i are the track parameters and V_{ij}^{s} are the elements of the error matrix of the secondary vertex fit as defined in Chapter 3 (Tracks Vertices and Decay Lengths). The J/ψ and ϕ mass are calculated in a similar way with a sum over 2-tracks. The mass is calculated while constraining the four tracks to originate from a common point in space and with the dimuon pair to have the mass of the J/ψ. The invariant mass along with many other kinematical quantities of interest is written event by event into a vector-array (PAW ntuple). This procedure is repeated for every event. The following cuts are then made to to demonstrate a signal:

- The probability P(χ^2) for 6 degrees of freedom must be greater than 0.02 for Run-Ia, and greater than 0.01 for the combined Run-Ia-Run-Ib analysis. The difference between these two requirements is negligible.

- $\mid M_{K^+K^-} - M_\phi \mid$ <0.01 GeV, where $M_{K^+K^-}$ is the calculated invariant mass of the 2-kaon tracks and M_ϕ is the world average ϕ mass of 1.01943 GeV [32].

- The transverse momentum of the ϕ, $P_t(\phi)$ is greater than 1.25 GeV, other cuts of greater than 2 and 3 GeV are used to remove background when making lifetime measurements. The aforementioned requirement is sufficient to demonstrate a signal in the mass spectrum.

An invariant mass plot of $B_s^0 \rightarrow J/\psi\phi$ is shown with a lifetime cut of $c\tau$ >100 μm in Fig. 4.1.

4.2 Reconstruction of $B_d^0 \rightarrow J/\psi K^*(892)^0$

The decay chains for $B_d^0 \rightarrow J/\psi K^*(892)^0$ are $J/\psi \rightarrow \mu^+\mu^-$ and $K^{*0}(892) \rightarrow K^{\pm}\pi^{\mp}$. The method for reconstruction of the J/ψ is identical to that described in the previous subsection and the only difference with the previous decay mode is the presence of the K resonance instead of a ϕ. Since we cannot distinguish π's from K's the assignment of their masses to the two non-muon tracks is arbitrary, therefore the entire procedure for the B_s^0 is repeated assigning the first track the mass of the π and the second track the mass of the K. The event with the mass recalculated in this fashion is called a "duplicate" event. To remove the ambiguity the $K\pi$ combination closest to the $K^*(892)^0$ in mass is chosen. The following cuts are used to produce the invariant mass distribution:

- The probability of the four-track vertex fit P(χ^2) is > 0.01.

- $\mid M_{K^{\pm}\pi^{\mp}} - M_K \mid$ is < 100 GeV where $M_{K^{\pm}\pi^{\mp}}$ is the calculated invariant mass of the K resonance.

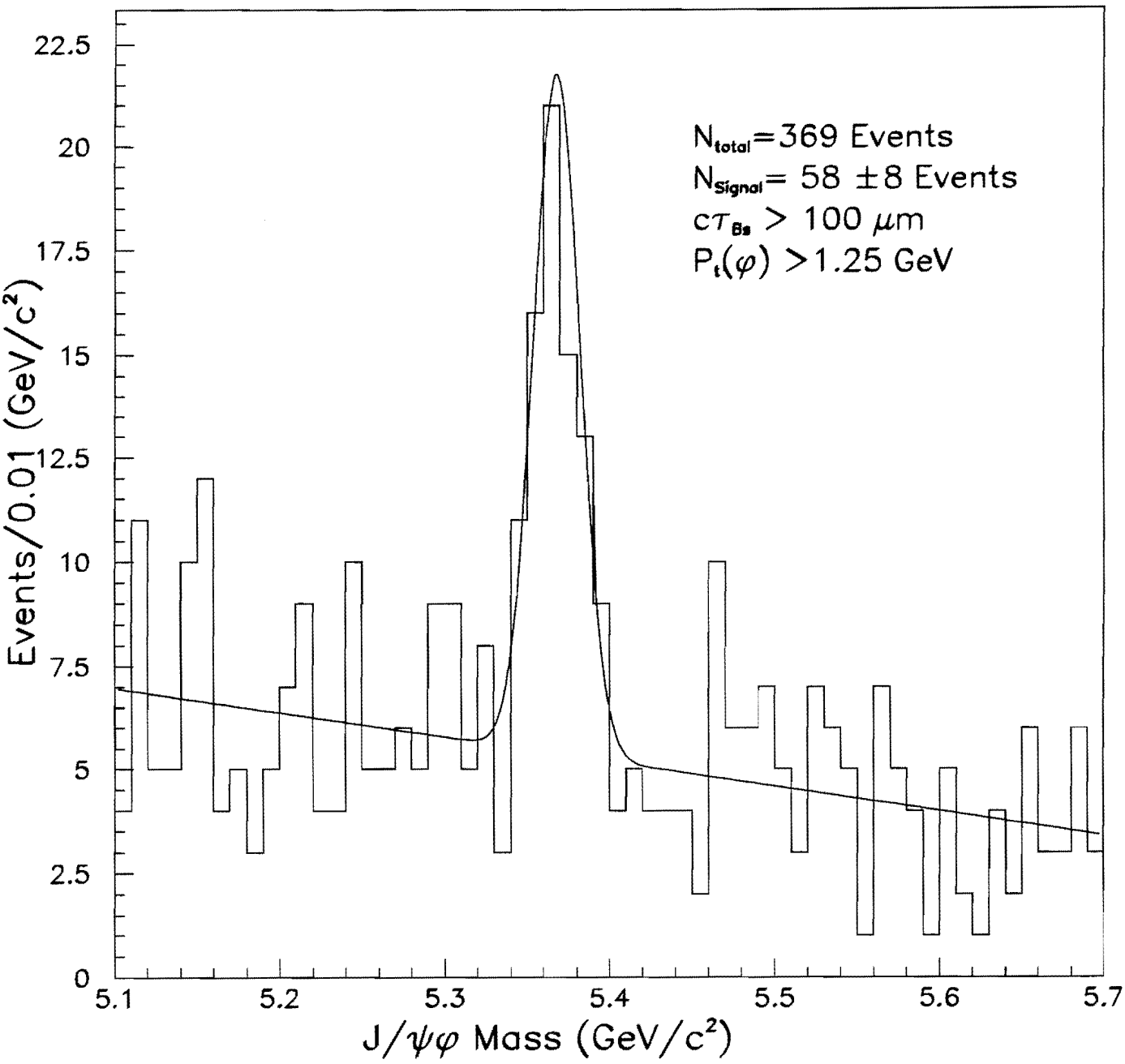

Figure 4.1:

The B_s^0 invariant mass distribution is displayed for $P_t(\phi) > 1.25$ GeV and $c\tau > 100$ μm.

- The transverse momentum of the K, $P_t(K)$ is > 2.0 GeV, other harder cuts are used to remove background when making lifetime measurements. The aforementioned requirement is sufficient to demonstrate a signal in the mass spectrum.

The masses and the errors on mass are calculated as given in Eqns. 4.1 and 4.2. Results for the lifetime are given for both decay modes in Chapter 5.(Determination of Lifetimes).

Chapter 5

Determination of Lifetimes

In this Chapter a description of the fitting technique used for determining lifetimes is given. The method described has not been used by any other CDF analysis and was developed during the Run-Ia analysis as a result of difficulties encountered in fitting data with low statistics. Both the mass and lifetime spectra are fit simultaneously to determine the mean lifetime and mass of the B_s^0.

5.1 Maximum Log-Likelihood Method

The maximum log-likelihood method has been used for determining the best fit lifetime. The likelihood function is defined as the log of the product of the normalized probabilities of each of the N events used. Since the mass and the proper-decay length spectra are fit simultaneously, each term $f_i(x_i, m_i)$ in the expression below is the product of two individual probability densities depending on the value of the proper decay length and the invariant mass. The parameters describing these spectra

are varied until the function is maximized. The log-likelihood is given by

$$\mathcal{L} = \log(\prod_{i=1}^{N} f_i(x_i, m_i)), \tag{5.1}$$

where m_i (Chapter four) is the invariant mass and x_i is the proper-decay length (Chapter three) of the ith event. In practice the quantity $-\mathcal{L}$ is minimized.

5.2 The Signal $c\tau$ Distribution

The probability distribution function for the measured proper-decay length of a the B_s^0 is an exponential decay function. However, there is an error on each proper-decay length and therefore the probability distribution function $F_s(x_j, \sigma_j, \lambda_{B_s^0})$ is modeled by an exponential decay function convoluted by a Gaussian resolution function. This is given by

$$F_s(x_j, \sigma_j, \lambda_{B_s^0}) = \frac{1}{\sqrt{2\pi}\sigma_j \lambda_{B_s^0}} \int_0^\infty e^{\frac{-(t-x_j)^2}{2\sigma_j^2}} e^{\frac{-t}{\lambda_{B_s^0}}} dt, \tag{5.2}$$

where the standard deviation of this Gaussian σ_j is the error calculated on the measured proper decay length x_j, and t is the actual point where the decay took place. The calculation of σ_j and x_j is described in Chapter three. Expressing the above in terms of the error function the probability distribution function of jth measured proper decay length x_j is given by

$$F_s(x_j, (s\sigma_j), \lambda_{B_s^0}) = \frac{1}{2\lambda_{B_s^0}} e^{\frac{(s\sigma_j)^2}{2\lambda_{B_s^0}^2} - \frac{x_j}{\lambda_{B_s^0}}} [1 - \mathrm{erf}(\frac{(s\sigma_j)}{\sqrt{2}\lambda_{B_s^0}} - \frac{x_j}{\sqrt{2}(s\sigma_j)})], \tag{5.3}$$

where $\lambda_{B_s^0}$ is the mean proper-decay length of the B_s^0. A scale factor for the error s is also introduced to account for a possible scaling of errors in the data. The mean

lifetime of the B_s^0 is $\tau = \frac{\lambda_{B_s^0}}{c}$. In the case where a cut is made on the measured proper decay length x_j, only a portion of the x_j distribution is fitted and in order to do this the above distribution must be normalized to the region $x_j > \kappa$, where $\kappa > 0$. This is done by determining the normalization N from the integral

$$N \int_{\kappa}^{\infty} F_s(x_j, (s\sigma_j), \lambda_{B_s^0}) dx_j = 1, \tag{5.4}$$

The correctly normalized function with a cut on the measured lifetime is given by

$$F_s(x_j, (s\sigma_j), \lambda_{B_s^0})_{cut=\kappa} = \frac{\frac{1}{2\lambda_{B_s^0}} e^{\frac{(s\sigma_j^2)}{2\lambda^2_{B_s^0}} - \frac{x_j}{\lambda_{B_s^0}}} [1 - \mathrm{erf}(\frac{(s\sigma_j)}{\sqrt{2}\lambda_{B_s^0}} - \frac{x_j}{\sqrt{2}(s\sigma_j)})]}{1 + e^{\frac{(s\sigma_j)^2}{2\lambda^2_{B_s^0}} - \frac{x_j}{\lambda_{B_s^0}}} - [e^{\frac{-\kappa}{\lambda_{B_s^0}}} \mathrm{erf}(\frac{(s\sigma_j)}{\sqrt{2}\lambda_{B_s^0}} - \frac{\kappa}{\sqrt{2}(s\sigma_j)}) - \mathrm{erf}(\frac{-\kappa}{\sqrt{2}(s\sigma_j)})]} \tag{5.5}$$

There are two free parameters in the function describing the shape of the signal proper decay length distribution. Of these s the scale factor for the errors is also a free parameter in the function describing the shape of the background. The free parameters in the signal function are heretofore referred to as the components of the vector $\vec{S}_s$.

5.3 The Background $c\tau$ Distribution

In its most general parameterization, the background is assumed to have three components, a zero-lifetime (prompt) component described by a Gaussian, a long-lived positive-lifetime component which is an exponential decay function convoluted with a Gaussian, and a negative exponential decay function to describe events with negative lifetime. The probability-distribution function for the jth background event $F_b(x_j)$ is

given by

$$F_b(x_j) = (1 - f_+ - f_-)\frac{e^{\frac{-(x_j - \bar{x}_0)^2}{2(s\sigma_j)^2}}}{\sqrt{2\pi}(s\sigma_j)} + \frac{f_+}{2\lambda_+} e^{\frac{(s\sigma_j)^2}{2\lambda_+^2} - \frac{x_j}{\lambda_+}} [1 - \mathrm{erf}(\frac{(s\sigma_j)}{\sqrt{2}\lambda_+} - \frac{x_j}{\sqrt{2}(s\sigma_j)})] + \frac{f_-}{\lambda_-} e^{\frac{x_j}{\lambda_-}} \tag{5.6}$$

where x_j is the measured proper decay length and σ_j is its calculated uncertainty and the parameters describing the shape of the background are given below:

i. f_+ is the fraction of positive-lifetime events in the background.

ii. λ_+ is the lifetime of the positive-lifetime events.

iii. f_- is the fraction of negative-lifetime tail events in the background.

iv. λ_- is the lifetime of the negative-lifetime tail.

v. $\bar{x}_0$ is the mean of the Gaussian representing the prompt component of the background.

vi. s is an overall scale factor used for scaling the errors σ_j on the proper decay length $c\tau$.

In case a cut of $c\tau > \kappa$ (where $\kappa > 0$) is made on the x_j distribution the form for the shape of the background function is given by

$$F_b(x_j) = \frac{N(1 - f_+)}{\sqrt{2}s\sigma_j} e^{\frac{-(x_j - x_0)^2}{(s\sigma_j)^2}} + \frac{\frac{f_+}{2\lambda_+} e^{\frac{(s\sigma_j)^2}{2\lambda_+^2} - \frac{x_j}{\lambda_+}} [1 - \mathrm{erf}(\frac{s\sigma_j}{\sqrt{2}\lambda_+} - \frac{x_j}{\sqrt{2}s\sigma_j})]}{1 + e^{\frac{(s\sigma_j)^2}{2\lambda_+^2} - \frac{x_j}{\lambda_+}} - [e^{\frac{-\kappa}{\lambda_+}} \mathrm{erf}(\frac{s\sigma_j}{\sqrt{2}\lambda_+} - \frac{\kappa}{\sqrt{2}s\sigma_j}) - \mathrm{erf}(\frac{-\kappa}{\sqrt{2}s\sigma_j})]}, \tag{5.7}$$

where the factor of N multiplying the first term is the normalization for a Gaussian cut off at $x_j > \kappa$ and

$$N = \frac{1}{0.5(1 + \mathrm{erf}\frac{|\kappa - x_0|}{\sqrt{2}\sigma_j})}. \tag{5.8}$$

Since a cut of $c\tau > \kappa$ has been made, the negative lifetime tail is no longer present in the background and is therefore not included in Eqn. 5.7. In the B_s^0 analysis a cut on the proper-decay length was not required to isolate a signal, however this technique has been tried as a consistency check and is not recommended since the fit does not converge when the fraction of long-lived background is allowed to float. It is recommended for use only in analyses where there is no choice and the only way to isolate a signal is to cut on $c\tau$.

There are 6 free parameters describing the shape of the background distribution in proper decay length. Of these s, the scale factor for the errors is also a free parameter in the signal function. Heretofore the parameters describing the shape of the background proper-decay length distribution are denoted as the components of the vector $\vec{S}_b$.

5.3.1 Bivariate Probability Distribution Function

The bivariate probability density function for a simultaneous mass and lifetime fit is given below

$$f(x_j, m_j) = (1 - f_s)g(m_j)F_b(x_j, \vec{S}_b) + \frac{f_s}{\sqrt{2\pi}\sigma_{m_j}} e^{-\frac{(m_j - \bar{M}_B)^2}{2\sigma_{m_j}^2}} F_s(x_j, \vec{S}_s). \tag{5.9}$$

The function $F_s(x_j, \vec{S}_s)$ is the signal $c\tau$ probability distribution function, $F_b(x_j, \vec{S}_b)$ is the background probability distribution function, f_s is the fraction of events that are signal. The mass distribution is Gaussian with a mean of $M_{B_s^0}$ the mass of the B_s^0 meson, and σ_{m_j} the error of the jth calculated invariant mass. The dependence of both $F_s(x_j, \vec{S}_s)$ and $F_b(x_j, \vec{S}_b)$ on the scaled error $s\sigma_j$ on each x_j is understood. The function $g(m_j)$ is a second order polynomial describing the background mass distribution,

$$g(m_j) = p_0 + p_1 m_j + p_2 (m_j - \bar{M})^2, \tag{5.10}$$

there is one equation of constraint due to the normalization condition

$$\int_{m_1}^{m_2} g(m_j) dm_j = 1, \tag{5.11}$$

therefore the fit is done for p_1 and p_2 with p_0 expressed in terms of these two. The range $m_1 < m_j < m_2$ is the region in mass used for the fit. In the Run-Ia analysis the background in mass was assumed to be flat therefore,

$$g(m_j) = \frac{1}{m_2 - m_1}. \tag{5.12}$$

In the joint Run-Ia and Run-Ib analysis the second order polynomial in Equation 5.10 was used.

Since a negative log-likelihood fit is used the quantity minimized is

$$\mathcal{L} = -\log[\prod_{j=1}^{N} f(x_j, m_j)], \tag{5.13}$$

and the probability distribution function is normalized as,

$$\iint f(x_j, m_j)\, dx_j\, dm_j = 1 \tag{5.14}$$

The total number of free parameters in this method is 11.

5.4 Comparisons

5.4.1 An Alternate Likelihood Function

The charged-to-neutral B meson lifetime ratio (exclusive decays) analysis has utilized a different approach for making lifetime measurements. The invariant mass of B mesons is reconstructed using the same methods as described in Chapter 4 (Reconstruction) but the method used to fit the lifetime distribution is different. Only the $c\tau$ distributions are used and their shapes are parameterized exactly as in the mass and lifetime simultaneous fit method. A signal region is chosen from a mass window $\pm\ \Delta M_s$ around the world average B_d^0 or $B_u^{\pm}$ mass. A choice is made of two sideband regions of total width ΔM_b in mass. The lifetime spectrum of the events in the sideband is assumed to represent the shape of the background in the peak region. The number of observed events in both the peak and sideband regions are treated as variables distributed according to a Poisson distribution and the likelihood function includes the probability for the number of events in the sidebands to fluctuate up to the number of events observed in the peak region and vice-versa. The likelihood function is given by

$$\mathcal{L} = \frac{e^{-\bar{n_p}}\bar{n_p}^{n_p}}{n_p!}\frac{e^{-\bar{n_{bk}}}\bar{n_{bk}}^{n_{bk}}}{n_{bk}!}\prod_{j=1}^{n_p}(\alpha F_s(x_j,\vec{S}_s)+[1-\alpha]F_b(x_j,\vec{S}_b))\prod_{j=1}^{n_b}F_b(x_j,\vec{S}_b), \quad (5.15)$$

where the signal and background functions are exactly the same as in the mass lifetime simultaneous fit method. The following new quantities have been introduced in

equation 5.15:

i. n_p is the total number of observed events in the peak region.

ii. n_{bk} is the total number of observed events in the sideband region.

iii. α is the probability that any event in the peak region is signal.

iv. n_{sig} is the expected number of signal events in the peak region.

v. $\bar{n}_p$ and $\bar{n}_{bk}$ are the expected mean values of the number of events in the peak and sideband regions. These are calculated from

$$\bar{n}_p = \frac{n_{sig}}{\alpha}, \tag{5.16}$$

and

$$\bar{n}_{bk} = (\frac{n_{sig}}{\alpha} - n_{sig})\frac{\Delta M_b}{2\Delta M_s}. \tag{5.17}$$

The quantity that is actually minimized in the fit is $-\log(\mathcal{L})$. This method was developed by Schneider *et al.* [35] in the lifetime analysis of the exclusive decay modes of the B_d^0 and $B_u^{\pm}$ mesons.

5.4.2 A Comparison

Initially the Run-Ia analysis of the B_s^0 exclusive lifetime used the alternate method described in the previous subsection. However a large discrepancy was observed in the number of fitted signal events when compared with a fit of just the mass distribution. This method returned a significantly lower number of signal events. These problems

are documented elsewhere [34]. Due to this observed discrepancy the fit to the lifetime spectrum was then performed with the number of signal events fixed to the number returned from a fit of *just* the mass distribution. It was pointed out however that this method was incomplete because fixing the number of signal events could mean that a number of correlations were not being considered in this fit. Fixing the number of signal events does not take into account possible fluctuations in the signal or a possible correlation with the fraction of long lived background. The final method (published in Physical Rev. Letters) used in this thesis fits simultaneously the mass and lifetime [3]. In this method all correlations and information (including the shape of the mass distribution) are taken into account when fitting. A comparison of the two methods has been done to test both fitting methods using a toy Monte Carlo. A brief description of the testing procedure follows below.

A random number generator based on the Bays-Durham shuffle algorithm [36] is used to create a large number of fake data-sets generated according to the shape of the observed mass and lifetime distributions from the real data. All proper-decay lengths and masses are convoluted according to an event-by-event error modeled after the error distributions observed in the data. To mimic the current data set, 10000 fake data sets of 60 signal, and 800 background events were generated. The resulting distributions of fitted lifetimes have a different RMS for the two methods. The mass-lifetime simultaneous fit method has a spread of 46.4$\pm$0.4 μm and the alternative method has a RMS of 48.9$\pm$ 0.4 μm. Both methods return a mean within 2 μm of the generated mean. In samples where the Run-Ia data was simulated the alternate

method would not converge 30 % of the time. The mass-lifetime simultaneous fit method is therefore recommended for lifetime measurements in exclusive decay modes.

Chapter 6

Results

This chapter contains the results obtained from the fitting procedure described in the chapter five. To check the method the decay mode $B_d^0 \rightarrow J/\psi K^*(892)^0$ has also been analysed and the value of the B_d^0 lifetime has been found to be in good agreement with other measurements at CDF and around the world.

6.1 Lifetime of the B_d^0 in the decay mode $B_d^0 \rightarrow J/\psi K^*(892)^0$ as a cross-check

As a check of the procedure the B_d^0 lifetime has been fit in the decay mode $B_d^0 \rightarrow J/\psi K^*(892)^0$ which has higher statistics than $B_s^0 \rightarrow J/\psi\phi$. These results are presented in Tables 6.1 and 6.2. The tables contain the lifetime in units of μm. The value of the lifetime of the B_d^0 is $\tau_{B_d^0} = 1.60 \pm 0.11$ ps. This is in good agreement with the world average of $\tau_{B_d^0} = 1.57 \pm 0.05$ ps [1]. Figs. 6.1 and 6.3 contain plots of the lifetime spectra with the mass spectrum inset. The proper decay length distribution and fits are displayed on a logarithmic scale in Figs. 6.2 and 6.4. The fits have been done with cuts of $P_t(K^*(892)^0) > 2$ and 3 GeV. At least three of the four tracks are

required to be in the SVX. Note that the mass background has been assumed to be flat and is parameterized by equation 5.12.

Table 6.1: Fit parameters and results for the decay mode $B_d^0 \rightarrow J/\psi K^*(892)^0$ with $P_t(K^*(892)^0) > 2.0$ GeV. A mass window of 100 MeV on $K^*(892)^0$, at least 3 SVX tracks and mass window of $\pm$ 50 MeV on B_d mass of 5.279 GeV are required. The total number of events is 4192.

Parameter	Fit Value	Statistical Error
f_{signal}	0.0753	$\pm$0.0055
M_{B_d}	5.277 GeV	$\pm$0.001 GeV
λ_{B_d}	482 μm	$\pm 33\mu$m
x_0	3 μm	$\pm 2\mu$m
f_+	0.116	$\pm$0.0089
λ_+	221μm	$\pm 18\mu$m
$f_{c\tau_-}$	0.021	0.014
λ_-	354 μm	$\pm$ 211 μm
s	1.08	$\pm$ 0.08

Table 6.2: Fit parameters and results for the decay mode $B_d^0 \rightarrow J/\psi K^*(892)^0$ with $P_t K^*(892)^0 > 3.0$ GeV. A mass window of 100 MeV on $K^*(892)^0$, at least 3 SVX tracks and mass window of $\pm$ 50 MeV on B_d mass of 5.279 GeV are required. The total number of events is 1220.

Parameter	Fit Value	Statistical Error
f_{signal}	0.172	$\pm$0.0141
M_{B_d}	5.278 GeV	$\pm$0.001 GeV
λ_{B_d}	481 μm	$\pm 38\mu$m
x_0	3 μm	$\pm 2\mu$m
f_+	0.149	$\pm$0.0198
λ_+	276μm	$\pm 55\mu$m
$f_{c\tau\_}$	0.020	0.0060
$\lambda\_$	406 μm	$\pm$ 104 μm
s	1.029	$\pm$ 0.03

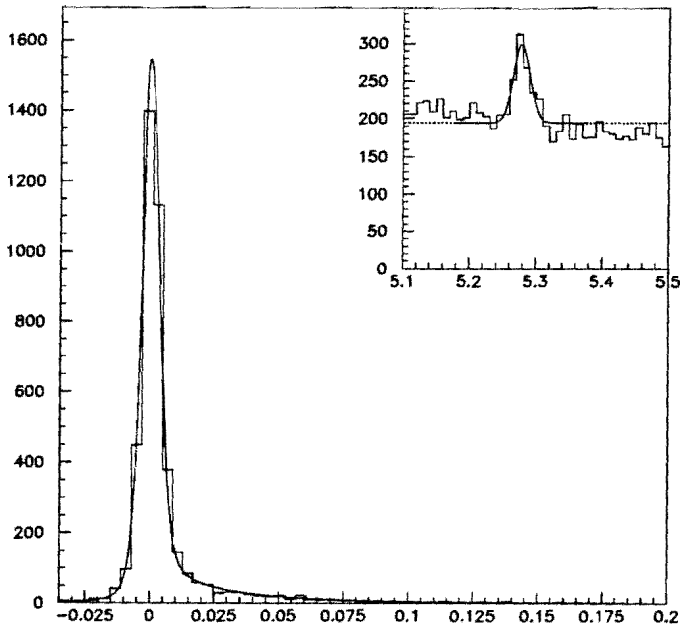

Figure 6.1:

The proper decay length distribution for the decay mode $B_d^0 \rightarrow J/\psi K^*(892)^0$ is shown for $P_t(K^*(892)^0) > 2$ GeV. The proper decay length histogram has 0.0040 cm (40 μm)bins and the inset mass distribution has 0.01 GeV bins.

6.2 Lifetime of the B_s^0 in the decay mode $B_s^0 \rightarrow J/\psi\phi$

The fit has been performed with 2 different P_t cuts and 4 different sets of requirements on the tracks to check for consistency:

i. Requiring the 2-muons in the SVX.

ii. Requiring any 3 tracks in the SVX.

iii. Requiring all 4 tracks in the SVX. Ideally this method uses the most accurately determined track parameters available, however the number of events passing this cut are few due to the partial coverage of the SVX.

iv. Only the SVX information of the muon tracks is used to determine the vertex (J/ψ only). Since the opening angle between the K^+ and K^- is very small the most accurate determination of the vertex is with the muon tracks.

The results are summarized in Table 6.3 given below.

Table 6.3: Fit parameters for the B_s^0 mass and lifetime distributions. The range in mass is 5.1–5.7 GeV. SVX requirements are varied.

$P_t(\phi)$	Tracks in SVX	Total	Signal	$c\tau_{B_s^0}$ (μm)
> 2.0	both muons	804	58 ± 8	402 ±61
> 2.0	any 3	877	61 ± 8	381 ±52
> 2.0	all 4 tracks	590	47 ± 7	360 ±58
> 2.0	J/ψ only	804	62 ± 9	386 ±59
>3.0	both muons	236	32 ± 6	479 ±92
>3.0	any 3 tracks	259	40 ± 6	461 ±78
>3.0	all 4 tracks	181	27 ± 5	484 ±98
>3.0	J/ψ only	236	31 ± 6	482 ±95

The fitted parameters for P_t cuts of >2 and 3 GeV which are used to make the plots are presented in Tables 6.4 and 6.5 respectively. For these final fits the 2-muons are required in the SVX.

Table 6.4: Fit parameters for the B_s^0 mass and lifetime distributions with a cut of $P_t(\phi) > 2$ GeV. The range in mass is 5.1–5.7 GeV. The total number of events is 804.

Parameter	Fit Value	Statistical Error
f_{signal}	0.072	$\pm$0.011
$\lambda_{B_s^0}$	402 μm	$\pm$61μm
x_0	2.1 μm	$\pm$1.6μm
f_+	0.103	$\pm$0.016
λ_+	297μm	$\pm$47μm
$f_{c\tau_-}$	0.0149	0.0051
λ_-	639 μm	214 μm
s	1.09	$\pm$ 0.04
$M_{B_s^0}$	5.364 GeV	$\pm$0.002 GeV
p_1	-0.368 GeV^{-2}	$\pm$0.379 GeV^{-2}
p_2	-6.176 GeV^{-3}	$\pm$2.207 GeV^{-3}

The first measurement of the B_s^0 lifetime in the decay mode $B_s^0 \rightarrow J/\psi\phi$ was made in Run-Ia with limited statistics; a value of $\tau_{B_s^0} = 1.74\ ^{+1.1}_{-0.6}$ (stat.) $\pm$0.07 (syst.) ps was published with $7.9\ ^{+3.6}_{-1.6}$ signal events. A plot of the mass and lifetime distributions

Table 6.5: Fit parameters for the B_s^0 mass and lifetime distributions with a cut of $P_t(\phi) > 3$ GeV. The range in mass is 5.1–5.7 GeV. The total number of events is 236.

Parameter	Fit Value	Statistical Error
f_{signal}	0.135	$\pm$0.0092
$\lambda_{B_s^0}$	479 μm	$\pm$92μm
x_0	0.3 μm	$\pm$3μm
f_+	0.152	$\pm$0.034
λ_+	371μm	$\pm$85μm
$f_{c\tau_-}$	0.0151	0.0095
λ_-	856 μm	54 μm
s	1.144	$\pm$ 0.0815
$M_{B_s^0}$	5.362 GeV	$\pm$0.003 GeV
p_1	-0.013 GeV^{-2}	$\pm$0.728 GeV^{-2}
p_2	-8.515 GeV^{-3}	$\pm$4.321 GeV^{-3}

is shown in Fig. 6.5. The combined Run-Ia and Run-Ib result is more significant with $\tau_{B_s^0} = 1.34\ ^{+0.23}_{-0.19}$ (stat.) $\pm$ 0.05 (syst.) ps (which is 402 $^{+68}_{-57}$ (stat.) $\pm$ 15 (syst.) μm) (Table 6.4). The fitted B_s^0 mass spectra for P_t cuts of 2 and 3 GeV are shown in Figs. 6.6 and 6.9 and the corresponding lifetime spectra are shown in Figs. 6.7 and 6.10. The fits to the proper decay length spectrum are shown on a log scale for P_t cuts of > 2 and 3 GeV in Figs. 6.8 and 6.11 respectively.

The value of $\tau_{B_s^0} = 1.34\ ^{+0.23}_{-0.19}$ (stat.) $\pm$ 0.05 (syst.) ps is calculated requiring 2 muons in the SVX and $P_t(\phi) > 2$ GeV.

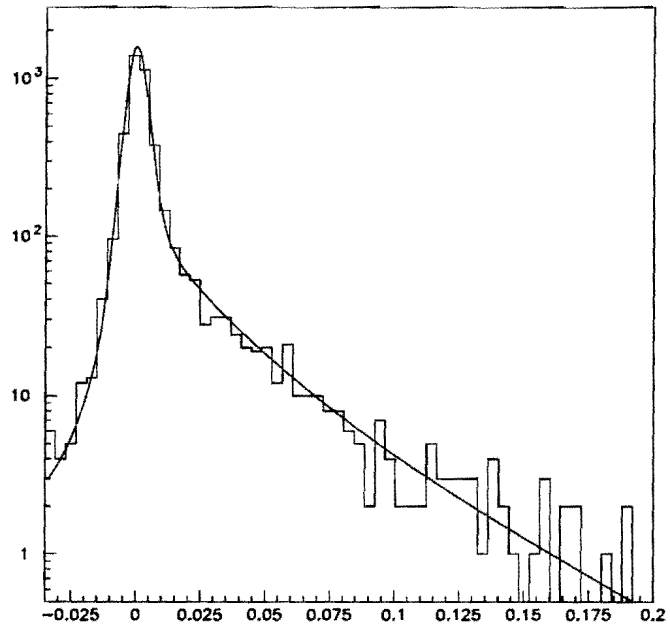

Figure 6.2:

The proper-decay length distribution for the decay mode $B_d^0 \rightarrow J/\psi K^*(892)^0$ is displayed on a logarithmic scale. The P_t of the $K^*(892)^0$ is greater than 2 GeV. The bin size is 0.0040 cm (40 μm).

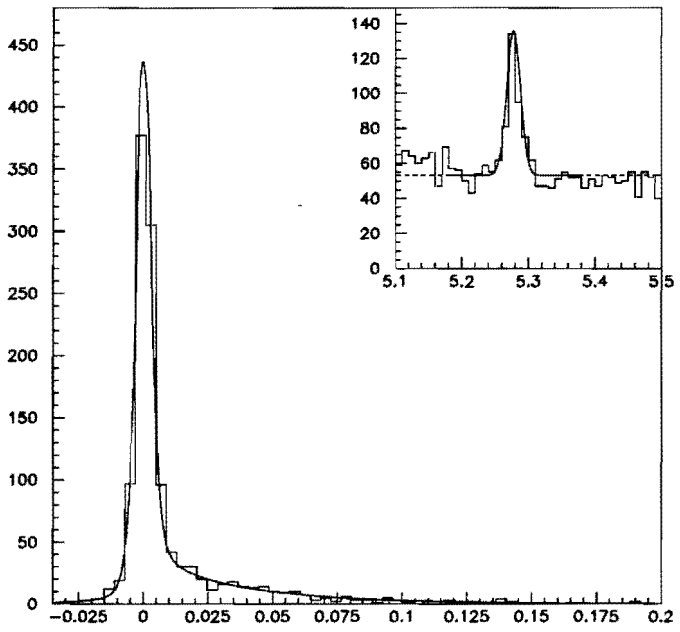

Figure 6.3:

The proper decay length distribution for the decay mode $B_d^0 \rightarrow J/\psi K^*(892)^0$ is shown for $P_t(K^*(892)^0) > 3$ GeV. The proper decay length histogram has 0.0040 cm (40 μm)bins and the inset mass distribution has 0.01 GeV bins.

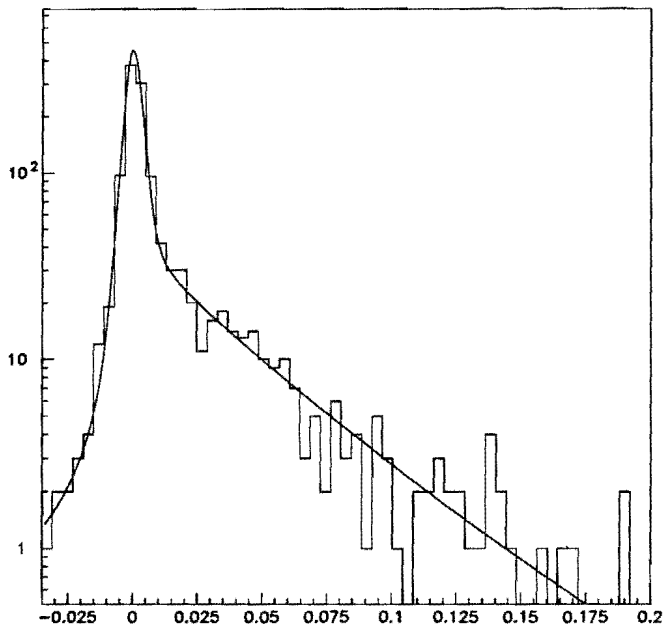

Figure 6.4:

The proper-decay length distribution for the decay mode $B_d^0 \rightarrow J/\psi K^*(892)^0$ is displayed on a logarithmic scale. The P_t of the $K^*(892)^0$ is greater than 2 GeV. The bin size is 0.0040 cm (40 μm).

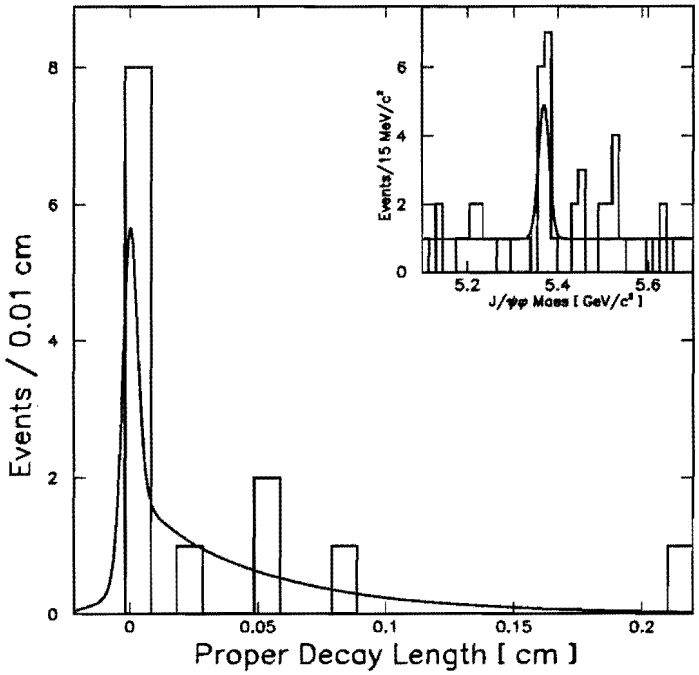

Figure 6.5:

B_s^0 proper decay length and mass (inset) distributions for $P_t(\phi) > 3$ GeV. Only Run-Ia data was used. This illustration was published in PRL [3].

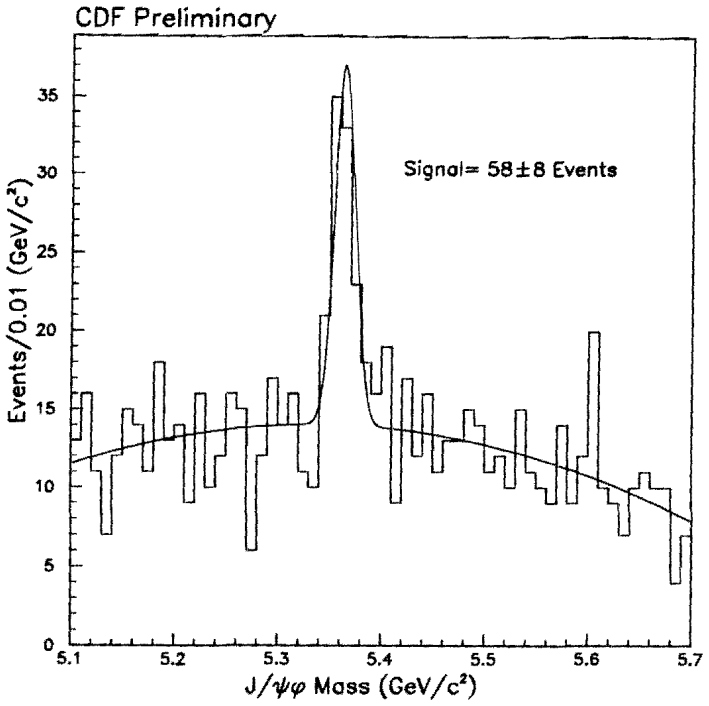

Figure 6.6:

The invariant B_s^0 mass distribution for $P_t(\phi) > 2$ GeV is shown fitted to a Gaussian and a polynomial background. The fit of this spectrum was performed simultaneously with fit of the $c\tau$ distribution in Fig 6.7.

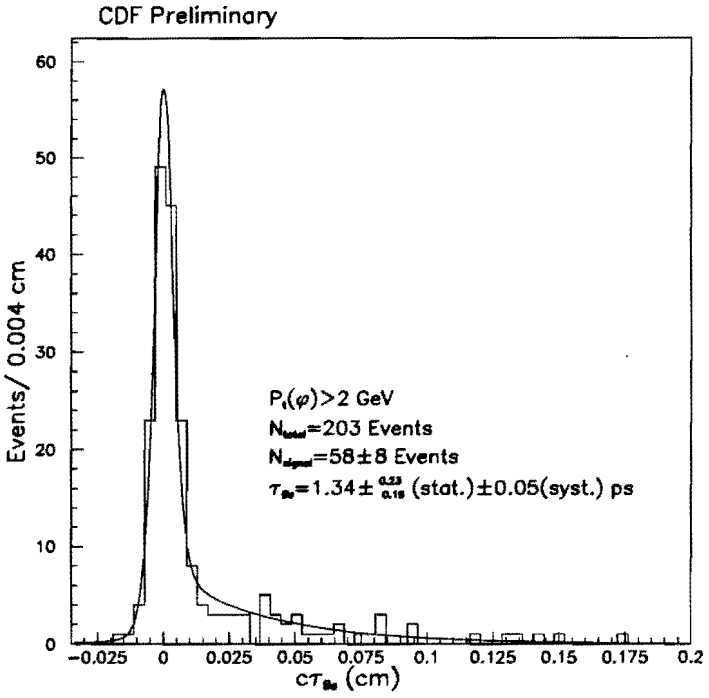

Figure 6.7:

B_s^0 proper decay length distribution for $P_t(\phi) > 2$. Events lying within a mass window of 5.363 $\pm$ 0.05 GeV are displayed.

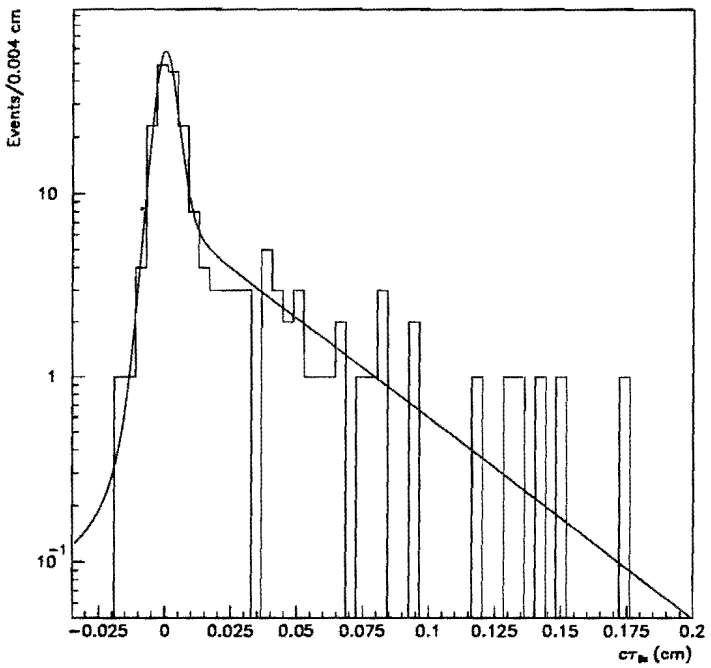

Figure 6.8:

B_s^0 proper decay length distribution for $P_t(\phi) > 2$. Events lying within a mass window of 5.363 ± 0.05 GeV are displayed on a logarithmic scale.

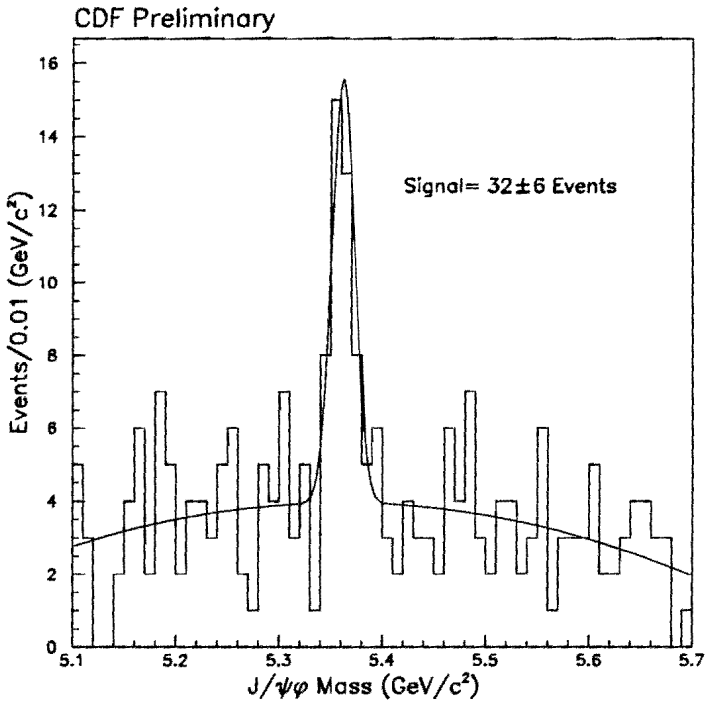

Figure 6.9:

The invariant B_s^0 mass distribution for $P_t(\phi) > 3$ GeV is shown fitted to a Gaussian and a polynomial background. The fit of this spectrum was performed simultaneously with the fit of the $c\tau$ distribution in Fig 6.10.

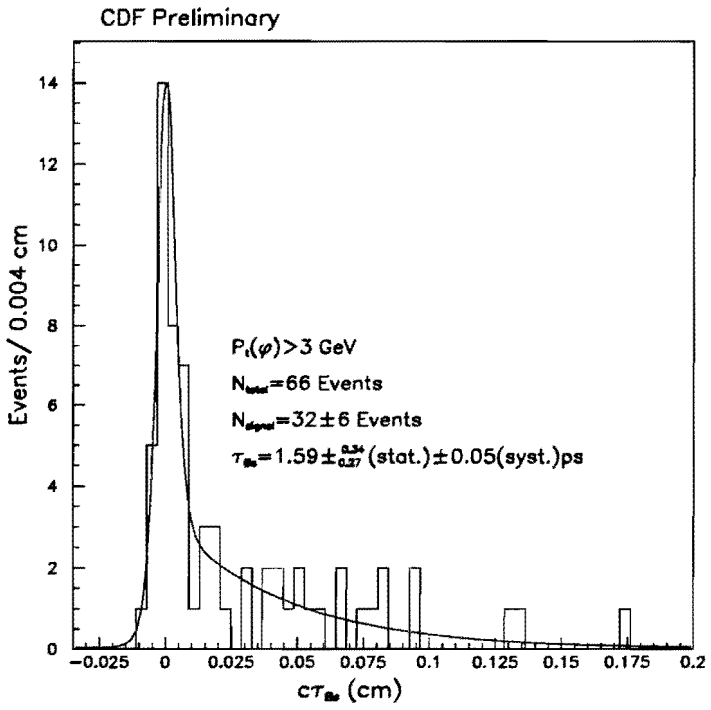

Figure 6.10:

B_s^0 proper decay length distribution for $P_t(\phi) > 3$. Events lying within a mass window of 5.363 $\pm$ 0.05 GeV are displayed.

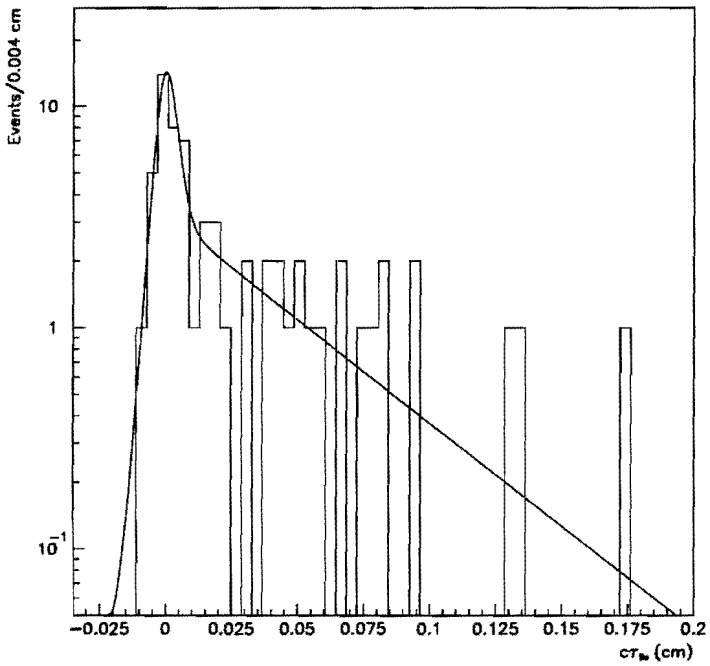

Figure 6.11:

B_s^0 proper decay length distribution for $P_t(\phi) > 3$. Events lying within a mass window of 5.363 ± 0.05 GeV are displayed on a logarithmic scale.

Chapter 7

Systematic Uncertainties

In this chapter the sources of systematic uncertainties for this lifetime measurement are discussed. The systematic errors in each category change very little from one run to the next. The decay mode $B_s^0 \rightarrow J/\psi\phi$ has lower statistics and the uncertainties at this stage are dominated by the statistical error.

7.1 Residual misalignment of the SVX

From the geometry and strip pitch of the SVX the intrinsic impact parameter resolution is known from Monte-Carlo to be ~ 13 μm. However there are two corrections that must be made when doing any data analysis:

- The alignment of the SVX relative to the rest of the CDF detector. (Global alignment)

- The alignment of various components of the SVX relative to one another. (Internal alignment).

To determine the effects of any *remaining* misalignments the following approach is utilized after the above alignments are done. $Z^0 \rightarrow l^+l^-$ decays are measured using tracks coming from the SVX. Since the lifetime of the Z_0, $\tau_{Z^0} \sim 0$, the sum of the signed impact parameters of the leptons should be 0. This quantity is plotted in Fig. 7.1 and the resulting distribution is shown fitted to a Gaussian. The σ of the Gaussian is the SVX resolution for measuring the sum of impact parameters of the 2 tracks and is = 23 μm. Thus the single track impact parameter resolution is taken to be $\frac{\sigma}{\sqrt{2}} = 16$ μm. At high energies $c\tau \sim d_0$, so that a systematic error of $\sqrt{16^2 - 13^2} \sim 10$ μm is assigned to residual misalignment of the SVX.

7.2 Trigger bias

The efficiency of the CFT Tracker varies with various kinematical quantities such as the P_t and the impact parameter d_0 of the tracks. The efficiency curve of the CFT for efficiency *vs* impact parameter was implemented in Monte-Carlo and the efficiencies are varied within errors to determine a possible systematic bias due to the trigger. This work has been done by Hans Wenzel *et al.* and work on a CDF internal note is in progress. The uncertainty is 6 μm in Run-Ia and 4 μm in Run-Ib.

7.3 Beam stability

Since the run-averaged beam position is used, it is neccesary to consider an uncertainty arising due to a shifting of the beam within a run. The average shift of a beam during a run has been reported elsewhere [37]. The variation in the position

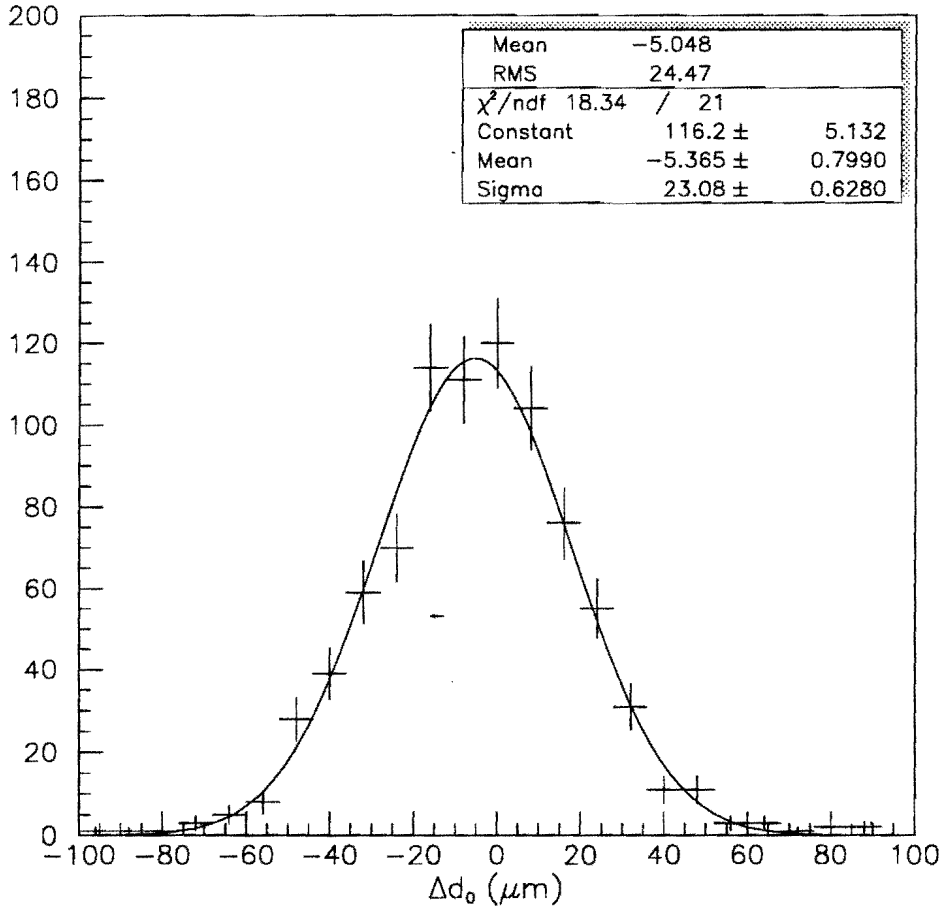

Figure 7.1:

Sum of the l^+l^- impact parameter distribution for $Z_0 \rightarrow l^+l^-$ decays. Resolution of the sum is 23 μm.

of the beam during a run is measured by calculating the beam position from several different groups of tracks within the same run. In Run-Ia this number was taken from the exclusive $B_d^0 - B_u^+$ analysis [35]. For Run-Ib the run-averaged beam position is replaced by a shifted beam position and the shift in lifetime is noted. The x-position is shifted by 5 μm and the y-position by 8μm. The beam position is offset by these amounts and the new lifetime is fitted. For the decay mode $B_s^0 \to J/\psi\phi$ the shift in lifetime in Run-Ib was 2 μm. In Run-Ia the number of 6 μm from the analysis of Schneider *et al.* [35] was used. In the combined Run-Ia and Run-Ib fit this shift is 2 μm.

7.4 Resolution function uncertainty

It is possible that the errors on the lifetime are correlated to the lifetime by an overall average scale factor s. To determine this scale factor a Gaussian is fit to the distribution of $\frac{c\tau}{\delta_{c\tau}}$ and the fit value of the standard deviation (σ) of this Gaussian is the scale factor. This number was 1.014$\pm$0.072 in Run-Ia, and is consistent with 1. The lifetime was then fit again while scaling $\delta_{c\tau}$ by $\sigma \pm \delta_\sigma$ and the deviations were recorded as a systematic uncertainty. A plot of the $\frac{c\tau}{\delta_{c\tau}}$ is shown in Fig. 7.2. In Run-Ib there are sufficient statistics to fit for this scale factor as a separate parameter. Thus the uncertainty in the lifetime due to variation in s is part of the statistical error. As a check, a fit of the $\frac{c\tau}{\delta_{c\tau}}$ distribution was made separately and was found to be consistent with the numbers returned from the fit of the B_s^0 lifetime. In the combined Run-Ia and Run-Ib fit this scale factor is fit along with other parameters and so it

is already included as part of the overall statistical error. This category is no longer listed separately in Run-Ib.

7.5 Background parameterization uncertainty

The parameterization of the background is described in Chapter 6 (Determination of Lifetimes). To assign an uncertainty due to a possible misparametrization of the background the shifts in the B_s^0 fitted lifetime due to a change in the shape fitted to the background $c\tau$ distribution were added in quadrature. The changes made and the shifts in lifetime due to each are listed below:

i. A flat contribution was added to the long-lived background and fitted for the fraction of events distributed flat in $c\tau$. This fraction converged to 0.0 with an error of $\pm$ 0.1. Then the flat-background fraction was fixed to 0.1 and the lifetime distribution was refit. The shift in lifetime was $\sim$14 μm in Run-Ia and 1 μm in Run-Ib.

ii. The positive long-lived background is usually modeled as an exponential decay function convoluted with a Gaussian resolution function. This was replaced with an exponential decay function and the lifetime distribution was fit again. The corresponding shift in lifetime was 1 μm in both runs.

iii. The mass distribution in the Run-Ia sample could only be fit with a flat background. In the combined Run-Ia and Run-Ib sample it is possible to use either a flat or polynomial background. The difference in lifetime from the two meth-

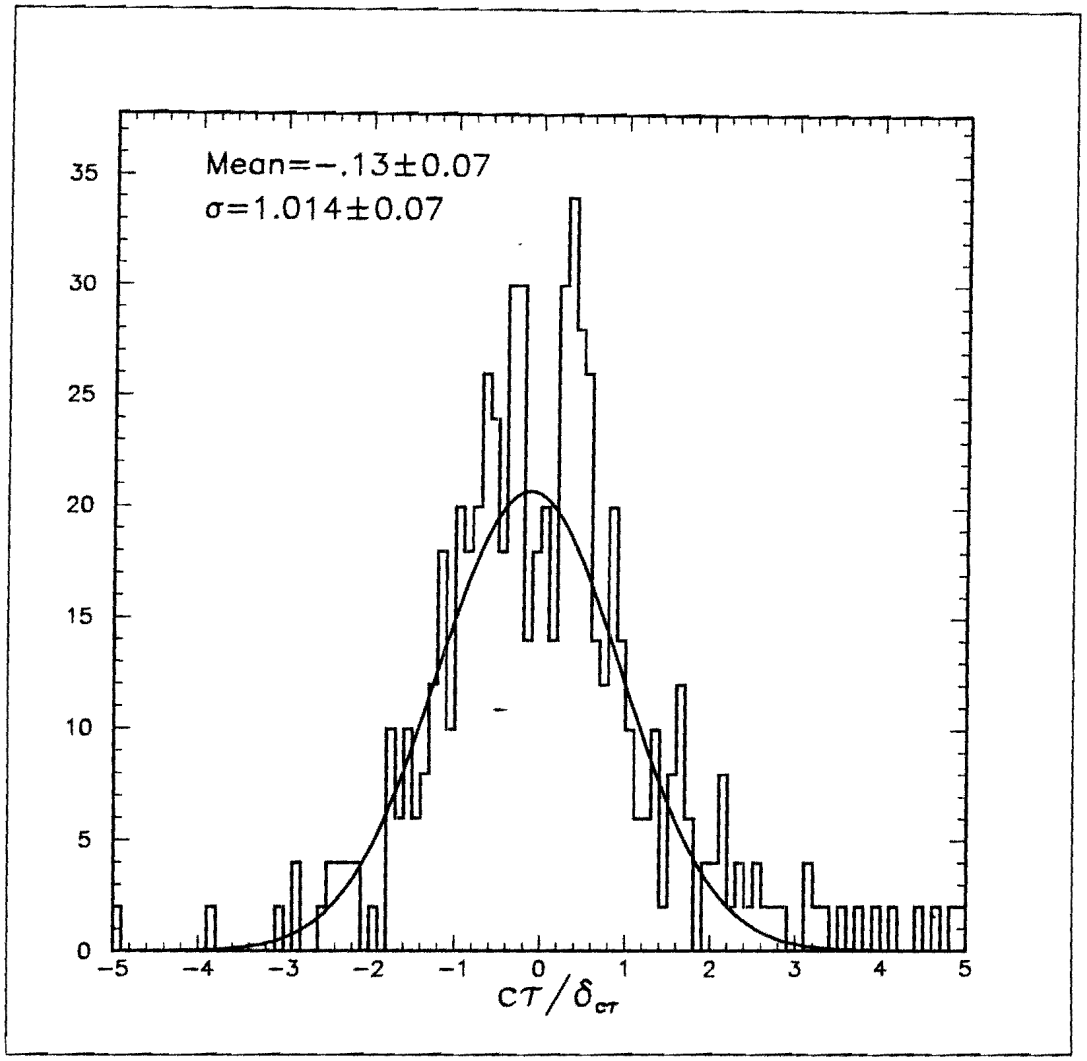

Figure 7.2: Determination of error scale for $B_s \to J/\psi\phi$ in the Run-Ia data sample, the distribution of $\frac{c\tau}{\delta_{c\tau}}$ is fit to a Gaussian. The fitted value of the standard deviation is the required scale factor for the errors.

ods is 10 μm. This is the largest source of uncertainty for the background parameterization category.

A total of 11μm is assigned to this category for the combined Run-Ia and Run-Ib fit. In Run-Ia this number was 14 μm.

7.6 Fitting Procedure bias

A sample of $\sim$ 10000 toy Monte-Carlo events modeled on the observed signal and background mass and lifetime distributions were generated (Chapter 5). The distributions were fit and the measured lifetime was recorded in each case. The mean was found to be shifted by ~ 2 μm from the generated lifetime. A systematic error of 2μm is therefore assigned to a possible bias of the fitting procedure used in this analysis.

7.7 Summary

Tables 7.1 and 7.2 given below summarize the sources of systematic errors for the Run-Ia and Run-Ib analyses. The sources as described above are beam stability, trigger bias, residual misalignment of the SVX, resolution function uncertainty and background parameterization in Run-Ia (Table 7.1). The resolution function uncertainty is not considered as a source of systematic uncertainty in Run-Ib since a scale factor for the errors is fit along with the other parameters. In Table 7.2 the categories of the Fitting Procedure and background parameterization have been recalculated for both runs. The differences in the other categories are still small enough that the total in quadrature (after rounding off) comes to 15 μm (0.05 ps). Therefore a total of

Table 7.1: A summary of the sources of systematic uncertainty for the decay mode $B_s^0 \to J/\psi\phi$ in Run-Ia.

Residual SVX misalignment	10 μm
Trigger bias	6 μm
Beam stability	5 μm
Resolution function uncertainty	6 μm
Background parameterization	14 μm
Total	20 μm

Table 7.2: A summary of the sources of systematic uncertainty for the decay mode $B_s^0 \to J/\psi\phi$ in Run-Ib.

Residual SVX misalignment	10 μm
Trigger bias	4 (Run-Ib only) μm
Beam stability	2 (Run-Ib only)μm
Fitting procedure bias	2 μm
Background parameterization	11 μm
Total	15 μm

15 μm or 0.05 ps is given as the final systematic uncertainty. A better alignment of the SVX can reduce the uncertainty due to residual misalignment from 10 to 5 μm. It is also expected that with more data (and a consequently better fit to the background) the uncertainty due to background parameterization will be reduced. A better understanding of systematic error will be crucial in Run-II as the statistical uncertainties will become comparable in size to the current systematic error.

Chapter 8

Conclusions

8.1 Summary of Lifetime Result

This thesis presents the first B_s^0 meson lifetime measurement in a fully reconstructed exclusive decay mode. The result of the measurement of the lifetime of the B_s meson is

$$\tau_{B_s^0} = 1.34\ ^{+0.23}_{-0.19}\ (\text{stat.})\ ^{+0.05}_{-0.05}\ (\text{syst.})\ \text{ps} \tag{8.1}$$

This is at present the most accurate measurement of the B_s^0 lifetime from any single source. The statistical error is the dominant uncertainty and is $\sim$ 16 %. As a consistency check, the B_d^0 lifetime has been measured to be

$$\tau_{B_d^0} = 1.60\ ^{+0.13}_{-0.10}\ (\text{stat.})\ \pm 0.05\ (\text{syst.})\ \text{ps}. \tag{8.2}$$

The result is in good agreement with the world average of 1.57 $\pm$ 0.05 ps [1].

8.2 Other Measurements of the B_s^0 Lifetime

The B_s^0 lifetime has been measured in inclusive decay modes at other experiments and at CDF. The inclusive decays used are $B_s^0 \rightarrow D_s l\bar{\nu}$ and $B_s^0 \rightarrow D_s^0 X$. Measurements

have been made at DELPHI [48], OPAL [45] and ALEPH [49] and CDF [3]. The world average B_s^0 lifetime based on these and the latest preliminary results is 1.58 $\pm$ 0.10 ps [1]. The measurement presented in this thesis is slightly lower but statistically consistent with each of these.

8.3 Implications for x_s

If the assumption is made that the decay $B_s^0 \rightarrow J/\psi\phi$ is dominated completely by the decay of the CP even state of the B_s^0 meson, it is possible to compute a value for the x_s mixing parameter. The world average B_s^0 lifetime from inclusive decays is used for the B_s^0 average lifetime. As stated earlier in Chapter one x_s is defined as

$$x_s = \frac{\Delta m}{\Gamma}. \tag{8.3}$$

The lifetime of the B_s^0 in a completely CP even decay mode allows us to calculate the ratio $\frac{\Delta\Gamma}{\Gamma}$ which is,

$$\frac{\Delta\Gamma}{\Gamma} = 2\frac{(\tau_{B_s^0 \text{ CPeven}} - \tau_{B_s^0 \text{ average}})}{\tau_{B_s^0 \text{ CPeven}}}, \tag{8.4}$$

and the ratio $\frac{\Delta m}{\Delta\Gamma}$ is calculable in terms of QCD parameters only. Therefore

$$x_s = \frac{\Delta m}{\Delta\Gamma}\frac{2(\tau_{B_s^0 \text{ CPeven}} - \tau_{B_s^0 \text{ average}})}{\tau_{B_s^0 \text{ CPeven}}}, \tag{8.5}$$

where

$$\frac{\Delta m}{\Delta\Gamma} \sim -\frac{2}{3\pi}\frac{m_t^2}{m_b^2}(1 - \frac{8}{3}\frac{m_c^2}{m_b^2})^{-1}h(\frac{m_t^2}{M_W^2}), \tag{8.6}$$

thus an expression for x_s is given by

$$x_s \sim -400\frac{\tau_{B_s^0 \text{ CPeven}} - \tau_{B_s^0 \text{ average}}}{\tau_{B_s^0 \text{ CPeven}}}. \tag{8.7}$$

If the B_s^0 world average lifetime from inclusives is used then $x_s = 72 \pm 55$.

8.4 The Future

The ratio of mixing in the $B_s^0 - \bar{B}_s^0$ system to that in the $B_d^0 - \bar{B}_d^0$ system is proportional to $\mid \frac{V_{ts}}{V_{td}} \mid^2$. Since $\mid V_{ts} \mid$ is expected to be $\sim 0.1 \mid V_{td} \mid$, the mixing parameter x_s is expected to be much larger than x_d [32]. The standard model can tolerate a lifetime as short as 1.46 ps corresponding to an x_s of 30 (95 % CL). The result presented in this thesis is consistent with the B_d^0 lifetime as well as a shorter B_s^0 lifetime. If a shorter lifetime is confirmed it could be due to 2 reasons:

- That the decay mode $B_s^0 \rightarrow J/\psi\phi$ is dominated by the CP even state of the B_s^0 and that the CP even state is shorter lived than the CP odd state.
- That there is no preponderance of either CP state in this decay but that the spectator model and the corrections fail in describing this decay mode accurately.

The errors on these measurements are large and it is hoped that data from Run-II (beginning in 1999) will allow a more precise measurement of this quantity. We estimate 2 fb^{-1} of data which is ~ 20 times larger than the current sample. Also a more efficient trigger and a greater acceptance in the SVX is expected to give us a factor of ~ 5. With a factor of a 100 increase in signal events in the decay mode $B_s^0 \rightarrow J/\psi\phi$ the statistical errors would be at the 2 % level. It is also expected that the systematic errors will be at the 1 % level. This combined with a 1 %

expected statistical error in the inclusive decay modes will allow us to measure a width difference, $\Delta\Gamma$, of significance ~ 5 if x_s is equal to its highest predicted value of 30.

References

[1] I. J. Kroll, "Masses and Lifetimes of B Hadrons", talk at the 17th International Symposium on Lepton-Photon Interactions. 11 August 1995.

[2] Thesis, Y.Cen title: "Measurement of the B_s Meson Lifetime".

[3] F.Abe *et al.* Phys. Rev. Lett. **74**, 4988 (1995).

[4] G.Altarelli *et al.* "Asymptotic Freedom in Parton Language", Nucl. Physics **B126** (1977) 298-318.

[5] J.C.Collins *et al.* "Heavy Flavour Production", Nucl. Physics (Proceedings Supplement) 12 1990, 219-225.

[6] Thesis, R.Hughes, title:"Reconstruction of B Meson Decays and the Measurement of the b Quark and B Meson Production Cross Section at the Fermilab Tevatron Collider".

[7] CDF Collaboration,"$J/\psi, \psi' \rightarrow \mu^+\mu^-$ and $B \rightarrow J/\psi, \psi'$ Cross Sections", Contributed paper to the 27th International Conference on High Energy Physics, Glasgow, July 20-27 1994.

[8] "Electron-Positron Annihilation Physics", B.Foster editor, (Adam Hilger, Bristol 1990).

[9] TASSO Collaboration, M. Althoff, *et al.* Z.Phys.C **27** 27 (1985).

[10] N.Lockyer *et al.* Phys. Rev. Lett **51**, 1316 (1983).

[11] E.Fernandez *et al.* Phys. Rev. Lett **51**, 1022 (1983).

[12] Jonathan Rosner, "Testing the Standard Model", Proceedings of the 1990 Theoretical Advanced Study Institute in Elementary Particle Physics.

[13] ARGUS Collaboration; Phys Lett. B **234**, 409 (1990).

[14] CLEO Collaboration; Phys Rev. Lett. **64**, 800 (1990).

[15] I.Bigi *et al.* "Non-Leptonic Decays of Beauty Hadrons From Phenomenology to Theory" CERN-TH-7132/1994.

[16] F.Ukegawa *et al.* "Measurement of the B^- and $\bar{B}^0$ Using Semi-leptonic Decays". Submitted to Phys.Rev.Letters.

[17] F.Abe *et al.* Phys. Rev. Lett. **72** 3456 (1994).

[18] P. Wells (OPAL Collaboration), invited talk in Heavy Flavour Physics session.

[19] A.Ali, D.London "CP-Violation and Flavour-Mixing in the Standard Model". DESY 95-148. UdeM-GPP-TH-95-32. Presented at the 6th Int. Symposium on Heavy Flavour Physics, Pisa, June 6-10 1995.

[20] Isard Dunietz '$B_s - \bar{B}_s$ Mixing, CP violation and Extraction of CKM Phases from Untagged B_s Data Samples' FERMILAB-PUB-94/361-T

[21] J.L. Rosner, Phys. Rev. **D 42**, 3732 (1990).

[22] F.Abe *et al.* Phys. Rev. Lett. **75** 3069 (1995).

[23] S.D. Holmes, " A Practical Guide to Modern High Energy Accelerators", Santa Fe TASI-87.

[24] S.D. Holmes, " Achieving High Luminosity in the Fermilab Tevatron", Fermilab CONF-91-341-E.

[25] D. Amedei *et al.* Nucl. Instr. and Meth. A289 (1990) 388.

[26] A. Datta *et al.* 'Are there B_s^0 Mesons with two Different Lifetimes', Phys. Lett. B, **196** 376 (1987).

[27] UA1 Collaboration, H.C. Albajar, *et al.* Phys. Lett. B **186** 247 (1987).

[28] Wenzel *et al.* 'Measurement of the Average Lifetime of B-Hadrons produced in $p\bar{p}$ collisions at $\sqrt{s}$= 1.8 TeV.' CDF internal note 2078.

[29] W.Wester *et al.* 'Measurement of the Mass of the B_s^0 Meson in $\bar{p}p$ Collisions at $\sqrt{s}$ =1.8 TeV' CDF internal note 3236. .

[30] P. Billoir *et al.* " Track Element Merging Strategy and Vertex Fitting in Complex Modular Detectors" Nucl. Instr. and Meth. **A241 (1985) 115-131**

[31] Hans Wenzel, " Tracking in the SVX ", CDF internal note 1970.

[32] Phys.Rev.D, Review of Particle Properties, **50**, 1173 (1994).

[33] Hans Wenzel, "Fitting the Beam Position with the SVX" CDF Internal Note 1924.

[34] F.Azfar *et al.* 'An Update on the B_s lifetime from the Decay $B_s^0 \rightarrow J/\psi\phi$ ' CDF internal note 2515.

[35] A.Spies *et al.* 'Measurement of B^+ and B^0 Lifetimes Using Exclusive Decay Channels', CDF internal note 2345.

[36] W.H. Press *et al.* "Numerical Recipes in Fortran" Cambridge University Press.

[37] J. Cammeretta *et al.* 'Run 1-B B^+ and B^0 Lifetimes Using Exclusive $B \rightarrow \psi K$ Decays' CDF internal note 3051.

[38] P.D.Acton *et al.* 'Measurement of the B_s Lifetime', Phys.Lett.B **312** pages 501-510 (1993).

[39] C.H. Wang *et al.* 'Alignment of the SVX' Using Run 1B Data' CDF internal note 3002.

[40] C.Peterson *et al.* "Scaling Violations In inclusive e^+e^- Spectra", Phys.Rev D, **Vol. 27** Number 1.

[41] CLEO Collaboration, E. H. Thorndike, Proc. 1985 Iny. Sym. on Lepton and Photom Interactions at High Energies, eds. M. Konumu and K. Takahashi(Kyoto,1986) p.406. ARGUS Collaboration, H. Albrecht et al.,Phys. Lett. B249(1990) 359

[42] M. B. Voloshin and M. A. Shifman, Sov. Phys. JETP 64 (1986) 698.
I. Bigi and N. Uraltsev, Phys. Lett. B 280 (1992) 271.

[43] ALEPH collaboration, CERN-PPE/93-42, Mar 1993.

DELPHI collaboration, CERN-PPE/92-174, Oct 1992.

OPAL collaboration, CERN-PPE/93-33, Feb 1993.

[44] F. Bedeschi *et al.*, CDF internal note 1987.

[45] OPAL collaboration, Phys. Lett. B **312** 501 (1993).

[46] S. L. Wu, Talk at Argonne Workshop, July 1993.

[47] Y. Cen *et al.* CDF internal note 1982.

[48] DELPHI Collaboration Zeit. Phys. **C61** 407.

[49] ALEPH Collaboration Phys. Lett. **B322** 441.